

Boundary operator expansion and extraordinary phase transition in the tricritical $O(N)$ model

Xinyu Sun¹ and Shao-Kai Jian^{2*}

¹ Institute for Advanced Study, Tsinghua University, Beijing 100084, China

² Department of Physics and Engineering Physics, Tulane University, New Orleans, Louisiana, 70118, USA

* sjian@tulane.edu

January 14, 2025

Abstract

We study the boundary extraordinary transition of a 3D tricritical $O(N)$ model. We first compute the mean-field Green's function with a general coupling of $|\vec{\phi}|^{2n}$ (with $n = 3$ corresponding to the tricritical point) at the extraordinary phase transition. Then, by employing the technique of layer susceptibility, we solve the boundary operator expansion using the $\epsilon = 3 - d$ expansion. Based on these results, we demonstrate that the tricritical point exhibits an extraordinary transition characterized by an ordered boundary for any N . This provides the first nontrivial example of continuous symmetry breaking in 2D dimensions in the context of boundary criticality.

Contents

1	Introduction	2
1.1	Summary of the results	4
2	Mean-field correlation functions at extraordinary transition	7
2.1	Mean-field order parameter profile	7
2.2	Mean-field two-point function	8
3	Order parameter and layer susceptibility	10
3.1	Order parameter profile	11
3.2	Layer susceptibility of the transverse modes	12
3.3	Layer susceptibility of the longitudinal mode	15
4	Boundary operator expansion	18
4.1	BOE of the transverse mode	18
4.2	BOE of the longitudinal mode	19
5	Extraordinary phase in tricritical $O(N)$ model	20
5.1	IR description of the extraordinary-log transition	20
5.2	Extraordinary transition at the tricritical point	22
6	Conclusion	25
A	Properties of special functions	25
A.1	Determination of integral constants $C_1^{L,T}$	25

A.2	Properties of regularized generalized hypergeometric function	26
B	Details of Feynman diagram calculation	26
B.1	Details of the evaluation for the integral $\int dp p^{d-2} I_\nu(pz) I_{\nu+1}(pz) K_\nu(pz') K_{\nu+1}(pz')$	26
B.2	Details of the evaluation for the integral I_1 and I_2	27
B.3	Details of the evaluation for the integral $I'_{1,2}$ and $I''_{1,2}$	30
C	Solution of the coupled RG equations Eq. (107)	32
D	Correlation function of the critical $O(N)$ theory	33
	References	34

1 Introduction

Boundary conformal field theory (BCFT) is a vibrant area of research with diverse applications across multiple disciplines [1]. The presence of a boundary enhances the bulk CFT by introducing additional conformal data [2–4]. For example, in BCFTs, bulk primary operators have a bulk-to-boundary operator product expansion (OPE) in addition to the standard bulk-to-bulk OPE. As a result, the two-point function in BCFT plays an important role, similar to the four-point function in CFT, as it admits different OPE channels, via a bulk OPE or via a boundary operator expansion (BOE) [3–6]. Note that this crossing symmetry is also the building block for conformal bootstrap in BCFTs [4].

In the boundary operator expansion channel, evaluating the two-point function can be technically simplified by transforming it into the layer susceptibility [7–9]. Specifically, there exists a one-to-one correspondence between the BOE of the two-point function and that of the layer susceptibility [3, 10, 11]. The layer susceptibility is more straightforward to compute perturbatively using Feynman diagrams, as it involves less intricate integrals. This approach is particularly advantageous at the extraordinary transition [12–15], where even the mean-field propagator becomes challenging to handle. For example, the BOE has been successfully computed in the $O(N)$ model at the extraordinary transition using layer susceptibility [10, 11]. This not only validates the critical exponents of the order parameter field but also unveils the spectrum of boundary operators.

The renewed interest in the extraordinary transition in three-dimensional $O(N)$ BCFT has been driven by the discovery of the extraordinary-log transition [16–22]. The BOE has predicted the existence of a critical flavor N_c , such that a logarithmic correlation function emerges at the boundary during the extraordinary transition when $2 \leq N < N_c$. However, beyond the critical $O(N)$ model [5, 23, 24], much remains unexplored. In this paper, we aim to extend the understanding of extraordinary transitions in three-dimensional BCFTs and investigate, in particular, continuous symmetry breaking in two dimensions (2D) in the context of boundary criticality. To achieve this, we compute the mean-field order parameter profile and propagator in an $O(N)$ field theory with a general $|\vec{\phi}|^{2n}$ coupling, providing a foundation for calculating the BOE in more general models. In the Appendix D, we rederive the BOE at the extraordinary transition in the critical $O(N)$ model, demonstrating the validity and versatility of our approach. To go beyond the critical $O(N)$ model, we focus on the extraordinary transition for $n = 3$, corresponding to the tricritical $O(N)$ model, the second most prevalent universality class in the $O(N)$ model [25–34]. Specifically, we derive the BOE at the one-loop level by cal-

culating the layer susceptibility, revealing the boundary operator spectrum. More inherently, because of the flowing of bulk-surface coupling parameter, we find that the boundary order parameter remains finite at the extraordinary transition of the tricritical $O(N)$ model for any N in three dimensions, in stark contrast to the extraordinary-log transition in the critical $O(N)$ model.

The paper is organized as follows. In the remainder of the introduction, we will briefly review the BOE of two-point functions, the layer susceptibility, and the relation between them. We then present a summary of our results, including the mean-field correlation function for general models and the BOE at the one-loop level for the tricritical model. Section 2 gives the detail of the evaluation for the mean-field correlation functions in the $O(N)$ field theory with a general $|\vec{\phi}|^{2n}$ coupling. In Section 3, we present a detailed evaluation of layer susceptibility, including the transverse and longitudinal parts, at the one-loop level via the $3 - \epsilon$ calculation. With the layer susceptibility, the BOE is obtained by series expansion of the hypergeometric function in Section 4, where the boundary operator content is discussed. Section 5 gives a brief review of the extraordinary-log transition. Importantly, we show that at strict $d = 3$ dimensions, because of the flow of coupling s , the boundary orders at extraordinary transition for all $N \geq 2$ in the tricritical $O(N)$ model. We conclude in Section 6 by discussing possible applications for our theory. Several appendices provide more details in the technical calculations. We also apply our general method to the critical $O(N)$ model with $|\vec{\phi}|^4$, by rederiving the BOE. The methods developed in this study lay a foundation for exploring BOEs in other models, and inspire investigations of boundary criticality at tricritical point. Broadly, we believe that it will also open avenues for further investigations into boundary criticality and its implications across diverse physical systems, such as topological systems [35–45] and holographic systems [46–53].

As mentioned in above, conformal symmetry implies the BOE of two point functions in terms of the boundary conformal block. Concretely, consider an $O(N)$ BCFT defined in a half-infinite space $z > 0$ with a boundary at $z = 0$. The connected two-point function of a primary scalar can be expressed by the boundary conformal block as follows [3, 4, 11],

$$G_{\text{con}}(r - r', z, z') = (4zz')^{-\Delta_\phi} \sum_{\Delta > 0} c_\Delta \sigma_\Delta \mathcal{G}_{\text{boe}}(\Delta, \xi), \quad (1)$$

$$\sigma_\Delta = 4^{-\Delta + \frac{d-1}{2}} \pi^{-\frac{d-1}{2}} \Gamma(\Delta) / \Gamma(\Delta - \frac{d-1}{2}), \quad \xi = \frac{(r - r')^2 + (z - z')^2}{4zz'}, \quad (2)$$

where r, r' is the coordinate in the subspace parallel to the boundary. Δ_ϕ denotes the scaling dimension of the primary field ϕ , and Δ is the scaling dimension of the boundary primary operators appeared in the BOE. The boundary conformal block, uniquely fixed by the conformal symmetry, $\mathcal{G}_{\text{boe}}(\Delta, \xi)$ is

$$\mathcal{G}_{\text{boe}}(\Delta, \xi) = \xi^{-\Delta} {}_2F_1\left(\Delta, \Delta + 1 - \frac{d}{2}, 2(\Delta + 1 - \frac{d}{2}); -\xi^{-1}\right). \quad (3)$$

The BOE coefficient is written as a product of c_Δ and σ_Δ because c_Δ is related to the BOE in layer susceptibility. The layer susceptibility is defined as

$$\chi(z, z') = \int d^{d-1}r G(r, z, z') = G(p = 0, z, z'), \quad (4)$$

where the coordinate variables in the subspace parallel to the boundary have been integrated out. This simplifies the calculations of the layer susceptibility. However, the layer susceptibility contains the full information about the BOE for the two-point function. It admits the following expansion,

$$\chi(z, z') = (4zz')^{\frac{d-1}{2} - \Delta_\phi} \sum_{\Delta > 0} c_\Delta \zeta^{\Delta - \frac{d-1}{2}}, \quad \zeta = \frac{\min(z, z')}{\max(z, z')}. \quad (5)$$

The relation between the BOE of the two-point function and the layer susceptibility is manifest in this expression as one can see that the BOE in layer susceptibility contains the expansion coefficient c_Δ as well as the same operator spectrum Δ . Hence, once the layer susceptibility is obtained, one is, in principle, able to extract the coefficient and the operator spectrum to construct the two-point function.

We consider the $O(N)$ model with a general coupling defined by the action,

$$S = \int_{z>0} d^{d-1}r dz \left[\frac{1}{2} |\nabla \vec{\phi}|^2 + \frac{u_0}{(2n)!} |\vec{\phi}|^{2n} + \frac{c_0}{2} |\vec{\phi}|^2 \delta(z) \right], \quad (6)$$

where u_0 denotes the strength of the self-coupling and c_0 denotes the mass at the boundary. $\vec{\phi} = (\phi_1, \dots, \phi_N)$ is a $O(N)$ field and $|\phi|^{2n} = \left(\sum_i \phi_i^2 \right)^n$. As we are interested in the extraordinary transition, $c_0 \rightarrow -\infty$, the order parameter does not vanish at the mean-field level, and we assume the ordered component to be ϕ_1 without loss of generality. We also consider the two-point function of the order parameter field, which will be separated into the transverse part, $G^T(r-r', z, z') = \langle \phi_i(r, z) \phi_i(r', z') \rangle$ where there is no summation for the index $i > 1$, and the longitudinal part, $G^L(r-r', z, z') = \langle \phi_1(r, z) \phi_1(r', z') \rangle$. Our contributions include the derivation of the mean-field correlation function for this general model, the layer susceptibility, and the BOE at the one-loop level for $n = 3$, corresponding to the tricritical $O(N)$ model. Additionally, we establish the extraordinary transition for any N in the tricritical $O(N)$ theory characterized by an ordered boundary, in stark contrast to the critical $O(N)$ theory. Below, we summarize our results.

1.1 Summary of the results

The mean-field order parameter profile, $m_0(z) \equiv \langle \phi_1(r, z) \rangle_0$ is

$$m_0(z) = \alpha(z + \beta)^{-1/(n-1)}, \quad (7)$$

with

$$\alpha = \left(\frac{(2n-1)! \cdot n}{(n-1)^2 u_0} \right)^{\frac{1}{2n-2}}, \quad \beta = -\frac{1}{(n-1)c_0}. \quad (8)$$

Because $c_0 < 0$ at the extraordinary transition, $\beta > 0$, and the order parameter profile is well-defined for $z \geq 0$. And $m_0(z \rightarrow \infty) = 0$ as expected for a vanishing order deep in the bulk. At the extraordinary fixed point, we can take $c_0 \rightarrow -\infty$, $\beta = 0$ to simplify the result.

Next, the mean-field two-point function in the mixed representation can be expressed by the modified Bessel function $K_\nu(x)$ and $I_\nu(x)$:

$$G_0^{L,T}(p, z, z') = \begin{cases} \sqrt{zz'} I_{\alpha_{L,T}}(pz') K_{\alpha_{L,T}}(pz), & z > z', \\ \sqrt{zz'} K_{\alpha_{L,T}}(pz') I_{\alpha_{L,T}}(pz), & z < z', \end{cases} \quad (9)$$

with $\alpha_L = \alpha_T + 1 = \frac{3n-1}{2(n-1)} = \frac{3}{2} + \frac{1}{n-1}$. From the two-point function, the mean-field layer susceptibility can be obtained straightforwardly via Eq. (4),

$$\chi_0^{L,T}(z, z') = \sqrt{zz'} \frac{\zeta^{\alpha_{L,T}}}{2\alpha_{L,T}}. \quad (10)$$

In the mean-field theory, the scaling dimension of the $O(N)$ field is $\Delta_\phi = \frac{d-2}{2}$. From the BOE in Eq. (5), one can see that $\Delta = \frac{d-1}{2} + \alpha_{L,T}$ and $c_\Delta = \frac{1}{4\alpha_{L,T}}$. It means that the corresponding longitudinal and transverse boundary modes have the scaling dimensions $\Delta_{L,T} = \frac{d-1}{2} + \alpha_{L,T}$, respectively.

The above discussion is on the general model. In the following, we will restrict to the tricritical $O(N)$ model with $n = 3$. The order parameter profile at the one-loop order is

$$m(z) = m_0(z) + m_1(z) = \left(\frac{90}{u_0}\right)^{\frac{1}{4}} z^{-\frac{1}{2}} \left[1 - \sqrt{\frac{5u_0}{8}} \frac{1+d}{5-d} + \frac{N-1}{5} \gamma_T z^{3-d} \right], \quad (11)$$

with $\gamma_T \equiv \frac{\Gamma(\frac{d+1}{2})\Gamma(\frac{2-d}{2})}{2^d \pi^{\frac{d}{2}} \Gamma(\frac{5-d}{2})}$. Notice that $\gamma_T < 0$ for $2 < d < 4$. The normalization of the one-point function can be obtained at the one-loop order,

$$m(z) = \frac{a_\sigma}{(2z)^{\Delta_\phi}}, \quad a_\sigma \approx \left(\frac{3(3N+22)}{8\pi^2}\right)^{\frac{1}{4}} \epsilon^{-\frac{1}{4}} + \frac{9+N}{2} \left(\frac{1}{6(3N+22)\pi^2}\right)^{\frac{1}{4}} \epsilon^{\frac{1}{4}}, \quad (12)$$

in which the fixed point of the coupling in Eq. (51) has been used. Strictly at $d = 3$, if we naively take $\epsilon = 0$ in a_σ , we will get an unphysical divergence for the order parameter. Instead, we should consider the logarithmic flow of the coupling in Eq. (57), which gives $m(z) \sim \frac{(\log \mu_0 z)^{1/4}}{z^{1/2}}$. The order parameter vanishes deep in the bulk $z \rightarrow \infty$ and receives a logarithmic correction, as expected at the upper critical dimension.

Now, we present the BOE of the layer susceptibility at the one-loop level. The transverse layer susceptibility reads,

$$\chi^T(z_1, z_2) = \sqrt{4z_1 z_2} \zeta^{-\frac{d-1}{2}} \sum_{\Delta=d-1, k} c_\Delta^T \zeta^\Delta. \quad (13)$$

with the expansion coefficient given by

$$\begin{aligned} c_{d-1}^T &= \frac{1}{4} - \frac{2 + 3c_{1,1} - 3c_{2,1}}{128\pi} \sqrt{\frac{u_0}{10}} = \frac{1}{4} - \frac{2 + 3c_{1,1} - 3c_{2,1}}{16} \sqrt{\frac{3}{2(3N+22)}} \epsilon^{\frac{1}{2}}, \\ c_k^T &= \frac{3}{8\pi} \frac{16}{k^2(k-1)(k-2)^2} \sqrt{\frac{u_0}{10}} = \frac{3}{2} \sqrt{\frac{6}{3N+22}} \frac{1}{k^2(k-1)(k-2)^2} \epsilon^{\frac{1}{2}}, \quad k = 5, 7, 9, \dots \end{aligned} \quad (14)$$

where $c_{1/2,1}$ is given by a complicated series. Their numerical value can be obtained as $c_{1,1} \approx -1.39608$ and $c_{2,1} \approx -1.48791$.

The primary boundary operator with scaling dimension of $d-1$ at both the leading and subleading order in the first line is related to the $O(N)$ conserved current that is broken at the boundary. It is also worth noting that in contrast to the ϕ^4 theory, the leading term in the ϵ expansion is $\mathcal{O}(\epsilon^{1/2})$. This is not a coincidence because the power of $\mathcal{O}(\epsilon^{1/2})$ also appears at the special transition [54].

The layer susceptibility for the longitudinal component is

$$\chi^L(z_1, z_2) = \sqrt{4z_1 z_2} \zeta^{-\frac{d-1}{2}} \sum_{\Delta=d, k} c_\Delta^L \zeta^\Delta. \quad (16)$$

with the following expansion coefficient,

$$\begin{aligned} c_d^L &= \frac{1}{8} + \frac{16 + 405(c'_{1,1} - c'_{2,1}) + 15(N-1)(c''_{1,1} - c''_{2,1})}{640} \frac{1}{8\pi} \sqrt{\frac{u_0}{10}} \\ &= \frac{1}{8} + \frac{16 + 405(c'_{1,1} - c'_{2,1}) + 15(N-1)(c''_{1,1} - c''_{2,1})}{640} \sqrt{\frac{3}{2(3N+22)}} \epsilon^{\frac{1}{2}} + \mathcal{O}(\epsilon). \end{aligned} \quad (17)$$

where the numerical values are $c'_{1,1} \approx -1.45699$, $c'_{2,1} \approx -1.35775$ and $c''_{1,1} \approx -1.64248$, $c''_{2,1} \approx -0.263237$. The operator with scaling dimension d is the displacement operator. The

presence of a boundary breaks the translation symmetry. As a result, the conservation of stress-energy tensor is violated by a boundary term, the displacement operator. Hence, its scaling dimension is protected to be d . Besides the displacement field, other boundary operators appeared in the BOE gives the coefficient,

$$\begin{aligned} c_4^L &= \frac{3}{16\pi} \frac{N-1}{(k-3)^2(k-1)(k+1)^2} \sqrt{\frac{u_0}{10}} \\ &= \frac{3}{2} \sqrt{\frac{3}{2(3N+22)}} \cdot \frac{N-1}{(k-3)^2(k-1)(k+1)^2} \epsilon^{\frac{1}{2}} + \mathcal{O}(\epsilon), \end{aligned} \quad (18)$$

$$\begin{aligned} c_k^L &= \frac{3}{16\pi} \frac{N+26}{(k-3)^2(k-1)(k+1)^2} \sqrt{\frac{u_0}{10}} \\ &= \frac{3}{2} \sqrt{\frac{3}{2(3N+22)}} \cdot \frac{N+26}{(k-3)^2(k-1)(k+1)^2} \epsilon^{\frac{1}{2}} + \mathcal{O}(\epsilon), \quad k = 6, 8, 10, \dots \end{aligned} \quad (19)$$

Again, we see the leading term in the ϵ expansion is $\mathcal{O}(\epsilon^{1/2})$.

Naively, setting $\epsilon = 0$ in the final expression of the expansion coefficients for $d = 3$ seems to indicate that BOE vanishes at the leading order. However, in strictly $d = 3$, u_0 is given by a logarithmic flow, $u_0 \sim \frac{1}{\log \mu_0 z}$. Substituting this logarithmic flow to the expression of BOE with explicit u_0 dependence in the first equality reveals that BOE has a logarithmic dependence instead of being completely trivial.

Lastly, we discuss the extraordinary transition. To explore the boundary order, we consider a coupled theory of the extraordinary (normal) transition model and the nonlinear sigma model:

$$S_{\text{IR}} = S_{\text{normal}} + S_n - s \int d^{d-1}r \sum_{i>1} \pi_i(r) \hat{t}_i(r), \quad (20)$$

$$S_n = \int d^{d-1}r \frac{1}{2g} (\partial_\mu \vec{n})^2, \quad (21)$$

where $\vec{n} = (\sqrt{1-\vec{\pi}^2}, \vec{\pi})$ and \hat{t}_i is the tilt field. s denotes the bulk-boundary coupling and g denotes the coupling in the nonlinear sigma model. The coupled RG equations of them are derived

$$\frac{ds}{d \log \mu} = -\frac{3(3N+22)}{128\pi^4} s^{-3}, \quad (22)$$

$$\frac{dg}{d \log \mu} = -\frac{N-2}{2\pi} g^2 + \frac{\pi s^2}{2} g^2. \quad (23)$$

with the solution being,

$$s \approx \left[\frac{3(3N+22)}{2(2\pi)^4} \log \mu_0 l \right]^{1/4}, \quad g \approx \frac{48(N-2)\pi}{3N+22} (\log \mu_0 l)^{-2} + \sqrt{\frac{96\pi^2}{3N+22}} (\log \mu_0 l)^{-3/2}. \quad (24)$$

where μ_0 is an arbitrary energy scale, and l denotes the length scale of the system. Notice that the logarithmic flow of coupling g is distinct from that in the critical $O(N)$ model: it decays faster than $(\log \mu_0 l)^{-1}$ at the long-wavelength limit. Consequently, we have the expectation value of the boundary order parameter at low energies,

$$\langle n \rangle_r \sim \exp \left[(N-1) \sqrt{\frac{24}{3N+22}} \left(\log \frac{\mu_0}{\sqrt{h}} \right)^{-1/2} \right], \quad h \rightarrow 0, \quad (25)$$

where h represents an external field linearly coupled to the surface order \vec{n} . We can see that as the external field h decreases to zero, the expectation of the surface order does not vanish! Hence, the tricritical point exhibits an extraordinary transition with an ordered boundary, in stark contrast to that in the critical $O(N)$ model. This can be understood intuitively, as the upper critical dimension for the tricritical point is $d = 3$, resulting in milder fluctuations compared to those at the critical $O(N)$ point. This provides a nontrivial example of continuous symmetry breaking in 2D dimensions within the context of boundary criticality [22].

2 Mean-field correlation functions at extraordinary transition

We consider an $O(N)$ model in a d -dimensional semi-infinite space, with the bulk (boundary) being $z > 0$ ($z = 0$). In this section, we will calculate the mean-field propagator at the extraordinary transition. We will give the result of mean-field Green's functions for an $O(N)$ model with a general coupling, as defined in the following action

$$S = \int_{z \geq 0} d^{d-1} r dz \left(\frac{1}{2} |\nabla \vec{\phi}|^2 + \frac{u_0}{(2n)!} |\vec{\phi}|^{2n} + \frac{c_0}{2} |\vec{\phi}|^2 \delta(z) \right). \quad (26)$$

Here, z denotes the coordinate perpendicular to the boundary surface which locates at $z = 0$, and r denotes the coordinate parallel to the boundary surface. $\vec{\phi} = (\phi_1, \dots, \phi_N)$ is an $O(N)$ field and u_0 denotes the self-coupling strength. Note that we consider a general $2n$ -th order coupling. c_0 is a boundary mass term. In general, boundary self-couplings should be considered. For instance, a boundary fourth order self-coupling should be considered at the special and ordinary transition for the tricritical $O(N)$ model. We will not consider the boundary self-coupling in this section for simplicity, and more importantly, we can show that all boundary self-couplings are irrelevant at the extraordinary transition for the tricritical $O(N)$ model.

In the following, we will give a derivation for the mean field order parameter profile and the mean field Green's function at the extraordinary transition. Before the derivation, we should note that while these results were derived for the ϕ^4 model [10], the results for $n \geq 3$ are new.

2.1 Mean-field order parameter profile

The mean-field order parameter profile and Green's function will then serve as a building block for our subsequent calculation for the layer susceptibility. We denote the order parameter profile as $m(z) \equiv \langle \phi_1(r, z) \rangle$ which does not depend on r due to the translational symmetry in the hypersurface parallel to the boundary surface. Note that we have taken the ordered to be ϕ_1 without loss of generality. Via a variational principle, the mean field equation for the order parameter is

$$-\frac{d^2}{dz^2} m_0(z) + \frac{u_0}{(2n-1)!} (m_0(z))^{2n-1} = 0, \quad (27)$$

with the boundary condition

$$\left(\frac{d}{dz} - c_0 \right) m_0(z) \Big|_{z=0} = 0. \quad (28)$$

The subscript is used to indicate the mean-field calculation. The solution for the extraordinary transition is

$$m_0(z) = \alpha(z + \beta)^{-1/(n-1)}, \quad (29)$$

with

$$\alpha = \left(\frac{(2n-1)! \cdot n}{(n-1)^2 u_0} \right)^{\frac{1}{2n-2}}, \quad \beta = -\frac{1}{(n-1)c_0}. \quad (30)$$

Because $c_0 < 0$ at the extraordinary transition, $\beta > 0$, and the order parameter profile is well-defined for $z \geq 0$. And $m_0(z \rightarrow \infty) = 0$ as expected for a vanishing order deep in the bulk. For $n = 2$, we have $\alpha = \sqrt{\frac{12}{u}}$ and $\beta = -\frac{1}{c_0}$. And the order parameter profile reads $m_0(z) = \sqrt{\frac{12}{u}} \left(z + \frac{1}{|c_0|}\right)^{-1}$. Then taking $c_0 \rightarrow -\infty$ gives results for the ϕ^4 theory [10].

2.2 Mean-field two-point function

Next, we shall derive the mean-field propagator on top of the mean-field order parameter profile. The Green's function will firstly be obtained in a mixed representation, namely, as a function of the momentum, p , conjugate to the coordinate parallel to the boundary surface and the position, z , away from the boundary. Moreover, there will be two distinct fluctuations away from the profile, namely, the transversal and the longitudinal fluctuations. As we will see, their corresponding Green's functions are also different. To proceed, we substitute the profile back into the action, then via a variational principle, the Green's function satisfies the following differential equation and boundary condition:

$$\begin{aligned} \left(-\frac{d^2}{dz^2} + p^2 + 2\frac{u}{(2n)!} C_{L,T} \cdot (m_0(z))^{2n-2}\right) G_0(p, z, z') &= \delta(z - z'), \\ \left(-\frac{d}{dz} + c_0\right) G_0(p, z, z')|_{z=0} &= 0, \end{aligned} \quad (31)$$

where $C_L = n(2n - 1)$ and $C_T = n$ for longitudinal and transverse fields and $m_0(z)$ is given in Eq. (29).¹ By taking $c_0 \rightarrow -\infty$, the differential equation can be simplified to

$$\left[-\frac{d^2}{dz^2} + p^2 + \left(\alpha_{L,T}^2 - \frac{1}{4}\right) z^{-2}\right] G_0(p, z, z') = \delta(z - z'), \quad (32)$$

with $\alpha_L = \alpha_T + 1 = \frac{3n-1}{2(n-1)} = \frac{3}{2} + \frac{1}{n-1}$.

To solve for the Green's function, we consider the corresponding homogeneous equation and make it dimensionless by variable $x = pz$,

$$\left[-\frac{d^2}{dx^2} + 1 + \left(\alpha_{L,T}^2 - \frac{1}{4}\right) x^{-2}\right] W(x) = 0. \quad (33)$$

Defining $W(x) = \sqrt{x}Q(x)$, it becomes

$$x^2 Q''(x) + xQ'(x) - \left(x^2 + \alpha_{L,T}^2\right) Q(x) = 0, \quad (34)$$

which is the standard modified Bessel equation, with two solutions being the modified Bessel function $I_\alpha(x)$ and $K_\alpha(x)$, $\alpha = \alpha_{L,T}$. Because we require $Q(x \rightarrow \infty) = 0$ for a physical solution, the suitable solution is $Q(x) \propto K_\alpha(x)$. Therefore, up to a constant prefactor, $W(x) = \sqrt{x}K_\alpha(x)$.² By standard technique [55], the solution for the Green's function can be expressed as

$$G_0(p, z, z') = \begin{cases} W_0(z, p)U(z', p), & z > z', \\ U(z, p)W_0(z', p), & z < z'. \end{cases} \quad (36)$$

¹Explicitly, C_L and C_T come from the prefactors of ϕ_1^2 and ϕ_i^2 , respectively, in the expansion of $((\phi_1 + m_0)^2 + \sum_{i>1} \phi_i^2)^n$.

²For $n = 2$, there is an elementary expression for the solution that

$$W_L(x) = e^{-x} \left(1 + \frac{3}{x} + \frac{3}{x^2}\right), \quad W_T(x) = e^{-x} \left(1 + \frac{1}{x}\right), \quad (35)$$

for longitudinal and transverse fields [30, 54]. The derivation also appeared in Refs. [7, 9].

Because z, z' are symmetric, we consider $z < z'$ without loss of generality. In this case, we have

$$U(z, p) = C_1 W_1(z, p) + C_2 W_2(z, p), \quad (37)$$

and we take $W_0(z, p) = W_1(z, p) = W(pz)$ and $W_2(z, p) = W(-pz)$. From the homogeneous solution, we have explicitly $W(pz) = W_{L,T}(pz) = \sqrt{pz} K_{\alpha_{L,T}}(pz)$ for the longitudinal and transversal component. The relative phase between $C_1^{L,T}$ and $C_2^{L,T}$ can be fixed by requiring $U(z \rightarrow 0, p)$ being finite: $C_2^{L,T} = -C_1^{L,T} e^{i\pi(\alpha_{L,T} - \frac{1}{2})}$ for the longitudinal and transversal component, respectively.

Next, the remaining overall constant $C_1^{L,T}$ can be determined by integrating z in Eq. (32) that leads

$$\frac{d}{dz} G(z \rightarrow z' - 0^+) - \frac{d}{dz} G(z \rightarrow z' + 0^+) = 1. \quad (38)$$

Plugging the general solution Eq. (36) into Eq. (38), for longitudinal mode G_L we have

$$1 = -C_1^L p e^{-i\frac{n\pi}{1-n}} \frac{ix}{2} \left[K_{\alpha_L}(x)(K_{\alpha_{L-1}}(-x) + K_{\alpha_{L+1}}(-x)) \right. \\ \left. + K_{\alpha_L}(-x)(K_{\alpha_{L-1}}(x) + K_{\alpha_{L+1}}(x)) \right], \quad (39)$$

where $x = pz'$. The r.h.s. can be simplified using the properties of special functions, as detailed in Appendix A.1, with the final result given by

$$1 = -\pi C_1^L p e^{-i\frac{n\pi}{1-n}}, \quad C_1^L = \frac{1}{\pi p} e^{i\frac{\pi}{1-n}}. \quad (40)$$

For transverse mode G_T , similarly, we have

$$C_1^T = \frac{1}{\pi p} e^{i\frac{n\pi}{1-n}}. \quad (41)$$

With integral constants $C_{1,2}^{L,T}$, Eq. (37) can be simplified as ($x = pz$)³

$$\pi p \cdot U_L = e^{i\frac{\pi}{1-n}} (W_L(x) - W_L(e^{i\pi}x) e^{-i\frac{n\pi}{1-n}}) = \pi \sqrt{x} I_{\alpha_L}(x), \\ \pi p \cdot U_T = e^{i\frac{n\pi}{1-n}} (W_T(x) - W_T(e^{i\pi}x) e^{-i\frac{\pi}{1-n}}) = \pi \sqrt{x} I_{\alpha_T}(x). \quad (42)$$

Finally, the Green's function in the mixed representation can be expressed by the modified Bessel function $K_\nu(x)$ and $I_\nu(x)$:⁴

$$G_0^{L,T}(p, z, z') = \begin{cases} \sqrt{zz'} I_{\alpha_{L,T}}(pz') K_{\alpha_{L,T}}(pz), & z > z', \\ \sqrt{zz'} K_{\alpha_{L,T}}(pz') I_{\alpha_{L,T}}(pz), & z < z'. \end{cases} \quad (43)$$

To derive the boundary operator expansion below, we can transform the Green's function to the layer susceptibility $\chi(z, z')$ [10, 11]. Assuming $z < z'$, we have

$$\chi_0^{L,T}(z, z') = \sqrt{zz'} \lim_{p \rightarrow 0} K_{\alpha_{L,T}}(pz') I_{\alpha_{L,T}}(pz) = \sqrt{zz'} \frac{1}{2\alpha_{L,T}} \left(\frac{z}{z'} \right)^{\alpha_{L,T}}, \quad z < z'. \quad (44)$$

For $z > z'$, we just need to exchange z and z' . Hence, with the variable $\zeta = \frac{\min(z, z')}{\max(z, z')}$, the mean-field layer susceptibility can be compactly expressed by

$$\chi_0^{L,T}(z, z') = \sqrt{zz'} \frac{\zeta^{\alpha_{L,T}}}{2\alpha_{L,T}}. \quad (45)$$

³Here we use the property for $K_\nu(x)$ that $K_\nu(e^{i\pi}x) = e^{-im\nu\pi} K_\nu(x) - i\pi \frac{\sin m\nu\pi}{\sin \nu\pi} I_\nu(x) \xrightarrow{m=1} e^{-i\nu\pi} K_\nu(x) - i\pi I_\nu(x)$.

⁴A similar expression has been shown in Ref. [56].

In the mean-field theory, the scaling dimension of the $O(N)$ field is $\Delta_\phi = \frac{d-2}{2}$. From the BOE in Eq. (5), one can see that $\Delta = \frac{d-1}{2} + \alpha_{L,T}$ and $c_\Delta = \frac{1}{4\alpha_{L,T}}$. It means that the corresponding longitudinal and transverse boundary modes have the scaling dimensions $\Delta_{L,T} = \frac{d-1}{2} + \alpha_{L,T}$, respectively.

In the following, we focus on the tricritical $O(N)$ model with $n = 3$. Setting $n = 3$ in Eq. (30), the mean-field order parameter profile is

$$m_0(z) = \left(\frac{90}{u_0}\right)^{1/4} z^{-1/2}. \quad (46)$$

The layer susceptibility is

$$\chi_0^L(z, z') = \sqrt{4zz'} \frac{\zeta^2}{8}, \quad \chi_0^T(z, z') = \sqrt{4zz'} \frac{\zeta}{4}, \quad (47)$$

where we have used $\alpha_T = \alpha_L - 1 = 1$ for $n = 3$. Finally, from the BOE, we can also get the mean-field Green's function according to the relation Eq. (1). With $\Delta_T = \Delta_L - 1 = \frac{d+1}{2}$, the mean-field Green's function is given by

$$\begin{aligned} G_0^L(r, z, z') &= (4zz')^{-\frac{d-2}{2}} \frac{1}{8} \frac{\Gamma(\frac{d+3}{2})}{16\pi^{\frac{d-1}{2}}} \xi^{-\frac{d+3}{2}} {}_2F_1\left(\frac{d+3}{2}, \frac{5}{2}, 5; -\xi^{-1}\right), \\ G_0^T(r, z, z') &= (4zz')^{-\frac{d-2}{2}} \frac{1}{4} \frac{\Gamma(\frac{d+1}{2})}{4\pi^{\frac{d-1}{2}}} \xi^{-\frac{d+1}{2}} {}_2F_1\left(\frac{d+1}{2}, \frac{3}{2}, 3; -\xi^{-1}\right). \end{aligned} \quad (48)$$

Notice that, here, we do not take $d = 3$ directly as we will implement the dimension regularization by setting $d = 3 - \epsilon$ in the next section.

3 Order parameter and layer susceptibility

In this section, we calculate the order parameter profile $m(z) = \langle \phi_1(z) \rangle$ and the correlation functions for the longitudinal and transverse modes up to the one-loop order.

At first, we briefly review the RG flow for the tricritical Ising model [54]. The bare coupling and the renormalized coupling are related via the renormalization factor Z_u , which in the one-loop order is given by

$$u_0 = Z_u u = \left(1 + \frac{1}{2\pi^2} \frac{3N + 22}{240} \frac{u}{\epsilon}\right) u, \quad (49)$$

where u_0 and u denote the bare and renormalized coupling constants, respectively. It leads to the following RG equation

$$\frac{du}{d \log \mu} = \beta_u, \quad \beta_u = -\epsilon u + \frac{1}{2\pi^2} \frac{3N + 22}{240} u^2. \quad (50)$$

There is a nontrivial IR fixed point, i.e., the tricritical $O(N)$ fixed point,

$$u^* = \frac{240}{3N + 22} \cdot 2\pi^2 \epsilon. \quad (51)$$

The field renormalization factor is trivial, $Z_\phi = 1$, in the one-loop order.

If $\epsilon = 0$, the solution to the RG equation is $u \sim \frac{1}{\log \mu_0 z}$ for large z , in which, μ_0 is an arbitrary momentum scale, and z plays the role of a length scale. Therefore, it corresponds to a logarithmic IR flow to the Gaussian fixed point, as expected at the upper critical dimension $d = 3$ for the tricritical theory. It is important to keep this logarithmic flow instead of directly setting $\epsilon = 0$ in the fixed point value of u^* . This was also emphasized in Ref. [10] in the context of the ϕ^4 theory.

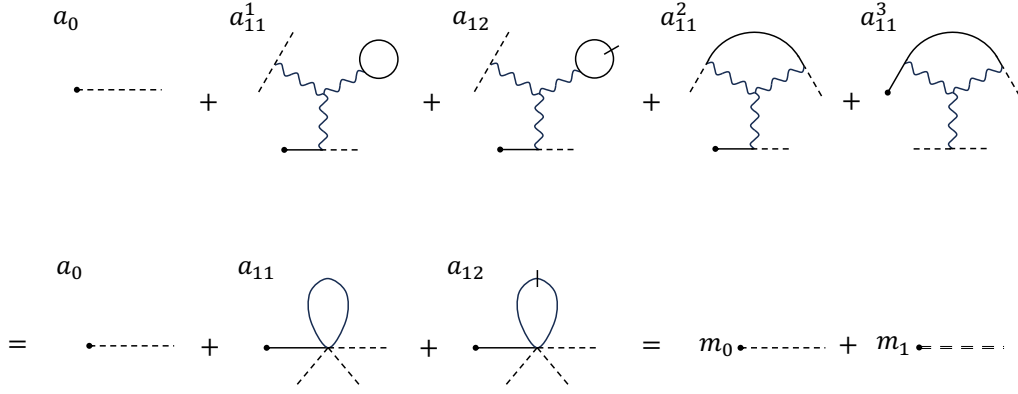


Figure 1: The Feynman diagram for magnetization $m(z) = \langle \phi_1(z) \rangle$. We use the dash line, wave line, and black dot to label $m_0 = \langle \phi_1(z) \rangle_0$, ϕ^6 vertex and $\phi_1(z)$. The solid line with (without) the short vertical line corresponds to the transverse (longitudinal) Green's function.

3.1 Order parameter profile

We consider the order parameter profile, $m(z) = \langle \phi_1(z) \rangle$, in the one loop order. The corresponding Feynman diagram is shown in Fig. 1. Here, we use a_{ij} to label a diagram with i numbers of vertices, for instance, a_{1j} (a_{2j}) denotes the Feynman diagram with a single vertex (two vertices). j in the subscript refers to the longitudinal or transversal loop as shown in Fig. 1. Contributions to a_{ij} may be further classified into different subdiagrams, which are labeled by superscript a_{ij}^k . It is clear from Fig. 1, and $a_{ij} = \sum_k a_{ij}^k$.

$m_0(z)$ and $m_1(z)$ correspond to the zeroth order and first order contributions to $m(z)$, respectively. The symmetry factor for the one vertex diagram in the first line of Fig. 1 respectively is 12, $12(N-1)$, 24 and 24 for a_{11}^1 , a_{12} , a_{11}^2 and a_{11}^3 . Therefore, we have $m(z) = m_0(z) + m_1(z)$ with $m_0(z) = a_0$, $m_1(z) = 60a_{11} + 12(N-1)a_{12}$, where a_{11} and a_{12} are

$$\begin{aligned} a_{11} &= \int d^{d-1}r dy \frac{-u_0}{6!} G_0^L(r_0 - r, z, y) (m_0(y))^3 G_0^L(r = 0, y, y), \\ a_{12} &= \int d^{d-1}r dy \frac{-u_0}{6!} G_0^L(r_0 - r, z, y) (m_0(y))^3 G_0^T(r = 0, y, y), \end{aligned} \quad (52)$$

with $G_0^{L,T}(r, z, z')$ being the propagator in Eq. (43). With the help of the layer susceptibility, they can be expressed as

$$\begin{aligned} a_{11} &= \int dy \frac{-u_0}{6!} \chi_0^L(z, y) (m_0(y))^3 G_0^L(r = 0, y, y), \\ a_{12} &= \int dy \frac{-u_0}{6!} \chi_0^L(z, y) (m_0(y))^3 G_0^T(r = 0, y, y). \end{aligned} \quad (53)$$

To proceed, recall that $\xi = \frac{(r-r')^2 + (z-z')^2}{4zz'}$, then from the Green's function Eq. (48), we have

$$\begin{aligned} G_0^L(r = 0, y, y) &= \frac{d+1}{5-d} \frac{\Gamma(\frac{d+1}{2})\Gamma(\frac{2-d}{2})}{2^d \pi^{\frac{d}{2}} \Gamma(\frac{5-d}{2})} y^{2-d} \equiv \gamma_L y^{2-d}, \\ G_0^T(r = 0, y, y) &= \frac{\Gamma(\frac{d+1}{2})\Gamma(\frac{2-d}{2})}{2^d \pi^{\frac{d}{2}} \Gamma(\frac{5-d}{2})} y^{2-d} \equiv \gamma_T y^{2-d}. \end{aligned} \quad (54)$$

Substituting this to a_{11} and performing the integration, we have

$$a_{11} = \frac{-u_0}{6!} \left(\frac{90}{u_0} \right)^{\frac{3}{4}} \frac{\gamma_L}{(4-d)d} z^{\frac{5}{2}-d}, \quad (55)$$

and similarly, a_{12} is given by replacing γ_L by γ_T . Finally, we have $m_1(z) = 60a_{11} + 12(N-1)a_{12}$:

$$m_1(z) = \frac{-u_0}{6!} \left(\frac{90}{u_0} \right)^{\frac{3}{4}} \frac{60\gamma_L + 12(N-1)\gamma_T}{(4-d)d} z^{\frac{5}{2}-d} = \frac{-u_0}{12} \left(\frac{90}{u_0} \right)^{\frac{3}{4}} \frac{\frac{d+1}{5-d} + \frac{N-1}{5}}{(4-d)d} \gamma_T z^{\frac{5}{2}-d}. \quad (56)$$

Hence, up to the first order, the order parameter profile is given by

$$\begin{aligned} m(z) &= m_0(z) + m_1(z) = \left(\frac{90}{u_0} \right)^{\frac{1}{4}} z^{-\frac{1}{2}} \left[1 - \sqrt{\frac{5u_0}{8} \frac{d+1}{5-d} + \frac{N-1}{5}} \gamma_T z^{3-d} \right] \\ &\equiv \left(\frac{90}{u_0} \right)^{\frac{1}{4}} z^{-\frac{1}{2}} \left[1 + \sqrt{u_0} c(\epsilon) z^\epsilon + \mathcal{O}(u^2) \right], \end{aligned} \quad (57)$$

where in the second line, we make the substitution $d = 3 - \epsilon$. Note that in the calculation, we have not considered the renormalization effect for the vertex itself. To incorporate the one-loop correction to the vertex, we substitute u_0 in Eq. (49) into Eq. (57) to get,

$$m(z) = \left(\frac{3(3N+22)}{16\pi^2} \right)^{\frac{1}{4}} \epsilon^{-\frac{1}{4}} z^{-\frac{1}{2}} \left\{ 2^{-\frac{1}{4}} + 4 \cdot 2^{\frac{3}{4}} \sqrt{\frac{15}{3N+22}} \pi c(\epsilon) z^\epsilon \epsilon^{\frac{1}{2}} + \dots \right\}, \quad (58)$$

where we have taken the fixed point value $u_0 = 2u^* = 4\pi^2 \frac{240}{3N+22} \epsilon$. Denoting the normalization of the one-point function by a_σ , namely, $m(z) = \frac{a_\sigma}{(2z)^{\Delta_\phi}}$, we have

$$a_\sigma \approx \left(\frac{3(3N+22)}{8\pi^2} \right)^{\frac{1}{4}} \epsilon^{-\frac{1}{4}} + \frac{9+N}{2} \left(\frac{1}{6(3N+22)\pi^2} \right)^{\frac{1}{4}} \epsilon^{\frac{1}{4}}, \quad (59)$$

where we have expanded the results w.r.t. ϵ .

There are a few remarks. (i) We should also multiply Z_ϕ because $m(z) = \langle \phi \rangle = \langle \phi_{\text{bare}} \rangle / \sqrt{Z_\phi}$, but here we have $Z_\phi = 1$ [54] in the one-loop order. (ii) The leading term in Eq. (59) comes from $m_0(z)$ with $u_0 = 2u^*$. (iii) Strictly at $d = 3$, if we naively take $\epsilon = 0$ in a_σ , we will get an unphysical divergence for the order parameter. Instead, we should consider the logarithmic flow of the coupling in Eq. (57), which gives $m(z) \sim \frac{(\log \mu_0 z)^{1/4}}{z^{1/2}}$. The order parameter vanishes deep in the bulk $z \rightarrow \infty$ and receives a logarithmic correction, as expected at the upper critical dimension.

3.2 Layer susceptibility of the transverse modes

We consider the two-point functions of the transverse mode $\langle \phi_i(z) \phi_i(z') \rangle$ with $i \neq 1$, in the one loop order. The corresponding Feynman diagrams are shown in Fig 2. Here, we use b_{ij}^k to denote the diagram with i number of vertices. The symmetry factor of b_{11}^1 , b_{12}^1 , b_{11}^2 , and b_{12}^2 in Fig. 2 (a) are, respectively, 12, $12(N-1)$, 24 and 12. In total, single-vertex diagrams lead to the contribution, $36b_{11} + 12N b_{12}$, where b_{11} and b_{12} are shown on the right-hand side of Fig. 2 (a) and given by

$$\begin{aligned} b_{11} &= \frac{-u_0}{6!} \int d^{d-1} r dy (m_0(y))^2 G_0^L(0, y, y) G_0^T(r_1 - r, z_1, y) G_0^T(r_2 - r, z_2, y), \\ b_{12} &= \frac{-u_0}{6!} \int d^{d-1} r dy (m_0(y))^2 G_0^T(0, y, y) G_0^T(r_1 - r, z_1, y) G_0^T(r_2 - r, z_2, y). \end{aligned} \quad (60)$$

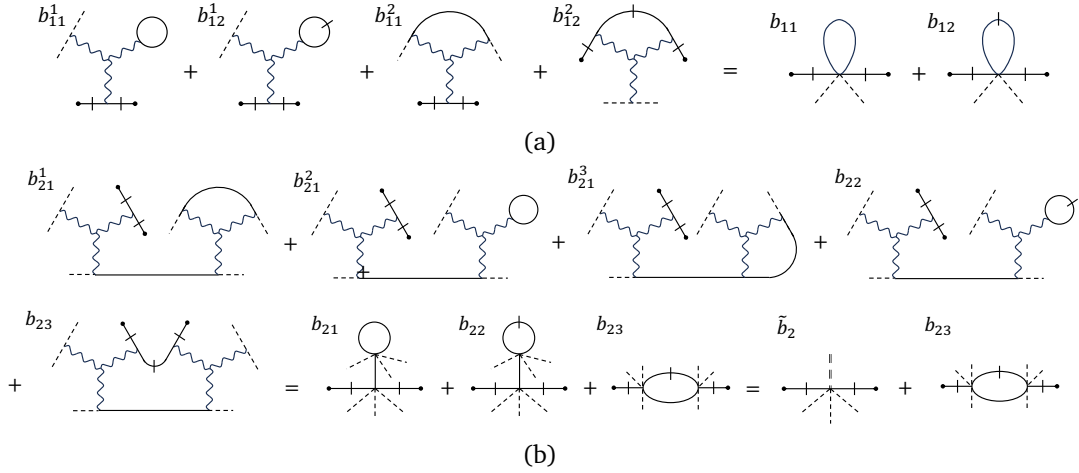


Figure 2: The Feynman diagram for Green's function of transverse modes $G^T(r - r', z, z') = \langle \phi_i(r, z) \phi_i(r', z') \rangle$. And $b_{ij} = \sum_k b_{ij}^k$. (a) The Feynman diagram with one vertex. (b) The Feynman diagram with two vertices. Here we combine b_{21} and b_{22} , and express it with $\tilde{b}_2(z)$.

Here and after, we will transform the Green's function to the layer susceptibility to simplify the calculations. After the calculation is completed, we can reconstruct the Green's function from the layer susceptibility using BOE detailed in the next section.

The corresponding layer susceptibility is denoted with $(\cdot)'$:

$$\begin{aligned} b'_{11} &= \int d^{d-1} r_2 b_{11} = \frac{-u_0}{6!} \int dy (m_0(y))^2 G_0^L(0, y, y) \chi_0^T(z_1, y) \chi_0^T(z_2, y), \\ b'_{12} &= \int d^{d-1} r_2 b_{12} = \frac{-u_0}{6!} \int dy (m_0(y))^2 G_0^T(0, y, y) \chi_0^T(z_1, y) \chi_0^T(z_2, y). \end{aligned} \quad (61)$$

The bare propagator and layer susceptibility are given in Eq. (48), and Eq. (47). We can directly perform the integration over y , and arrive at

$$\begin{aligned} b'_{11} &= \frac{-u}{6!} \int dy \left(\frac{90}{u} \right)^{\frac{1}{2}} y^{-1} \gamma_L y^{2-d} \sqrt{4z_1 y} \frac{1}{4} \frac{\min(z_1, y)}{\max(z_1, y)} \sqrt{4z_2 y} \frac{1}{4} \frac{\min(z_2, y)}{\max(z_2, y)} \\ &= \frac{\gamma_L \sqrt{\frac{u}{10}}}{48(d-5)(d-3)(d-1)} (z_1 z_2)^{\frac{4-d}{2}} \left((d-1) \zeta^{\frac{5-d}{2}} + (d-5) \zeta^{\frac{d-1}{2}} \right), \end{aligned} \quad (62)$$

where $\zeta = \frac{\min(z_1, z_2)}{\max(z_1, z_2)}$. Similarly, b'_{12} is obtained by replacing γ_L with γ_T .

Next, we calculate the two-vertex diagrams shown in Fig. 2 (b), denoted by b_{21}^1 , b_{21}^2 , b_{21}^3 , b_{22} , b_{23} . The symmetry factors are, respectively, 576, 288, 576, 288($N-1$) and 576. Combining them together, as shown in the middle expression in Fig. 2 (b), the two-vertex diagram leads to $1440b_{21} + 288(N-1)b_{22} + 576b_{23}$. Comparing $1440b_{21} + 288(N-1)b_{22}$ with m_1 in Fig. 1, we find that the loop in $1440b_{21} + 288(N-1)b_{22}$ can be expressed by $m_1(z)$. Effectively, $1440b_{21} + 288(N-1)b_{22} = 24\tilde{b}_2$ where we use $\tilde{b}_2 = 60b_{21} + 12(N-1)b_{22}$ to indicate the first diagram in the last equation of Fig. 2 (b). After a straightforward integration, the corresponding layer susceptibility is

$$\begin{aligned} \tilde{b}'_2 &= \frac{-u_0}{6!} \int dy (m_0(y))^3 \chi_0^T(z_1, y) \chi_0^T(z_2, y) m_1(y) \\ &= \frac{\gamma_T \sqrt{\frac{5u_0}{2}} \left(\frac{d+1}{5-d} + \frac{N-1}{5} \right)}{32(d-5)(d-4)(d-3)(d-1)d} (z_1 z_2)^{\frac{4-d}{2}} \left((d-1) \zeta^{\frac{5-d}{2}} + (d-5) \zeta^{\frac{d-1}{2}} \right). \end{aligned} \quad (63)$$

Now, let's focus on the calculation of b_{23} shown in the last diagram in Fig. 2 (b). The corresponding layer susceptibility reads

$$b'_{23} = \left(\frac{-u_0}{6!}\right)^2 \int dy_1 dy_2 \chi_0^T(z_1, y_1) \chi_0^T(z_2, y_2) (m_0(y_1))^3 (m_0(y_2))^3 B^{LT}(y_1, y_2), \quad (64)$$

where $B^{LT}(y_1, y_2) = \int d^{d-1}r G_0^T(r, y_1, y_2) G_0^L(r, y_1, y_2)$. We first calculate $B^{LT}(y_1, y_2)$. Using Fourier transformation in the hypersurface parallel to the boundary, we can use the mixed representation of Green's functions to simplify,

$$\begin{aligned} B^{LT}(y_1, y_2) &= \int \frac{d^{d-1}\vec{p}}{(2\pi)^{d-1}} G_0^T(\vec{p}, y_1, y_2) G_0^L(-\vec{p}, y_1, y_2) \\ &= \frac{S_{d-1}}{(2\pi)^{d-1}} \int dp p^{d-2} G_0^T(p, y_1, y_2) G_0^L(p, y_1, y_2) \\ &= \frac{S_{d-1}}{(2\pi)^{d-1}} y_1 y_2 \int dp p^{d-2} I_1(p y_1) K_1(p y_2) I_2(p y_1) K_2(p y_2), \end{aligned} \quad (65)$$

where $S_d = \frac{2\pi^{d/2}}{\Gamma(d/2)}$ is the area of a unit sphere in d dimension. In going from the second line to the last line, we used the bare propagator in Eq. (43) and assumed $y_1 < y_2$. The details of evaluation for the integral $\int dp p^{d-2} I_1(p y_1) K_1(p y_2) I_2(p y_1) K_2(p y_2)$ can be found in Appendix B.1. Taking $\nu = 1$ in Eq. (126), we have

$$\begin{aligned} B^{LT}(y_1, y_2) &= \frac{S_{d-1}}{(2\pi)^{d-1}} \frac{1}{4} y_1^{3-d} \left(\frac{y_1}{y_2}\right)^{d+1} \Gamma\left(\frac{d-1}{2}\right) \Gamma\left(\frac{5}{2}\right) \Gamma\left(\frac{d+1}{2}\right) \Gamma\left(\frac{d+5}{2}\right) \\ &\quad \times {}_4\tilde{F}_3\left[\left\{\frac{d-1}{2}, \frac{5}{2}, \frac{d+1}{2}, \frac{d+5}{2}\right\}, \left\{3, \frac{d+2}{2}, 4\right\}, \left(\frac{y_1}{y_2}\right)^2\right], \end{aligned} \quad (66)$$

in which ${}_p\tilde{F}_q$ is the regularized generalized hypergeometric function ${}_p\tilde{F}_q[a, b, z] = \frac{{}_pF_q[a, b, z]}{\Gamma(b_1)\cdots\Gamma(b_q)}$ with $a = \{a_1, \dots, a_p\}$ and $b = \{b_1, \dots, b_q\}$. For $y_1 > y_2$ we just exchange y_1 and y_2 in Eq. (66). With this result, b'_{23} can be simplified as follows,

$$\begin{aligned} b'_{23} &= \left(\frac{-u_0}{6!}\right)^2 \left(\frac{90}{u}\right)^{\frac{3}{2}} \frac{1}{4} \sqrt{z_1 z_2} \left(\int_0^\infty dy_1 \int_{y_1}^\infty dy_2 + \int_0^\infty dy_2 \int_{y_2}^\infty dy_1 \right) \frac{1}{y_1 y_2} \\ &\quad \times \frac{\min(z_1, y_1) \min(z_2, y_2)}{\max(z_1, y_1) \max(z_2, y_2)} B^{LT}(\min(y_1, y_2), \max(y_1, y_2)) \\ &\equiv \left(\frac{-u_0}{6!}\right)^2 \left(\frac{90}{u}\right)^{\frac{3}{2}} \frac{1}{4} \sqrt{z_1 z_2} \frac{S_{d-1}}{(2\pi)^{d-1}} \frac{1}{4} \Gamma\left(\frac{d-1}{2}\right) \Gamma\left(\frac{5}{2}\right) \Gamma\left(\frac{d+1}{2}\right) \Gamma\left(\frac{d+5}{2}\right) (I_1 + I_2), \end{aligned} \quad (67)$$

where $I_{1,2}$ are two integrals. The details of the evaluation for the integrals I_1 and I_2 can be found in Appendix B.2. Using the results in Eq. (131), b'_{23} is

$$b'_{23} = \frac{90^{\frac{3}{2}}}{(6!)^2} \frac{S_{d-1}}{32(2\pi)^{d-1}} \sqrt{u_0(z_1 z_2)^{\frac{4-d}{2}}} \left(AC_1 \zeta^{\frac{5-d}{2}} + BC_2 \zeta^{\frac{d-1}{2}} \right) + (z_1 z_2)^{\frac{4-d}{2}} H(\zeta), \quad (68)$$

where the constants C_1 and C_2 are given in Appendix B.2. Here we show the numerical value for these two constants in $\mathcal{O}(\epsilon)$

$$C_1 = \frac{4}{3} + c_{1,1}\epsilon + \mathcal{O}(\epsilon^2), \quad C_2 = \frac{4}{3} + c_{2,1}\epsilon + \mathcal{O}(\epsilon^2), \quad (69)$$

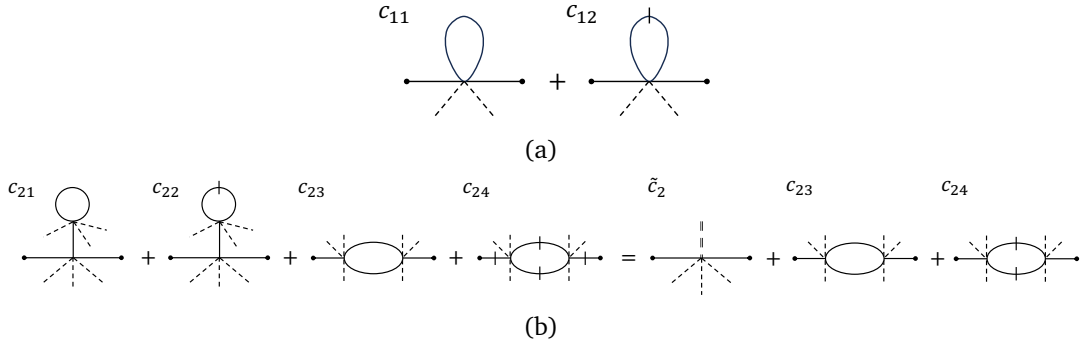


Figure 3: The Feynman diagram for Green's function of transverse modes $G^L(r - r', z, z') = \langle \phi_1(r, z) \phi_1(r', z') \rangle$. (a) The Feynman diagram with one vertex. (b) The Feynman diagram with two vertices. Here we combine c_{21} and c_{22} , and express it with $\tilde{c}_2(z)$.

where $c_{1,1} \approx -1.39608$ and $c_{2,1} \approx -1.48791$. And the last term is explicitly given by

$$\begin{aligned}
H(\zeta) = & \frac{90^{\frac{3}{2}}}{(6!)^2} \frac{S_{d-1}}{32(2\pi)^{d-1}} \Gamma\left(\frac{d-1}{2}\right) \Gamma\left(\frac{5}{2}\right) \Gamma\left(\frac{d+1}{2}\right) \Gamma\left(\frac{d+5}{2}\right) \sqrt{u_0} \zeta^{\frac{d+5}{2}} \\
& \left\{ A \Gamma\left(\frac{5}{2}\right) {}_5\tilde{F}_4 \left[\left\{ \frac{5}{2}, \frac{d-1}{2}, \frac{5}{2}, \frac{d+1}{2}, \frac{d+5}{2} \right\}, \left\{ \frac{7}{2}, 3, \frac{d+2}{2}, 4 \right\}, \zeta^2 \right] \right. \\
& - A \Gamma\left(\frac{d}{2}\right) {}_5\tilde{F}_4 \left[\left\{ \frac{d}{2}, \frac{d-1}{2}, \frac{5}{2}, \frac{d+1}{2}, \frac{d+5}{2} \right\}, \left\{ \frac{d+2}{2}, 3, \frac{d+2}{2}, 4 \right\}, \zeta^2 \right] \\
& + B \Gamma\left(\frac{d+2}{2}\right) {}_5\tilde{F}_4 \left[\left\{ \frac{d+2}{2}, \frac{d-1}{2}, \frac{5}{2}, \frac{d+1}{2}, \frac{d+5}{2} \right\}, \left\{ \frac{d+4}{2}, 3, \frac{d+2}{2}, 4 \right\}, \zeta^2 \right] \\
& \left. - B \Gamma\left(\frac{3}{2}\right) {}_5\tilde{F}_4 \left[\left\{ \frac{3}{2}, \frac{d-1}{2}, \frac{5}{2}, \frac{d+1}{2}, \frac{d+5}{2} \right\}, \left\{ \frac{5}{2}, 3, \frac{d+2}{2}, 4 \right\}, \zeta^2 \right] \right\}. \tag{70}
\end{aligned}$$

with $A = \frac{-2}{(d-5)(d-3)}$, $B = \frac{-2}{(d-3)(d-1)}$. It is obvious that for $d = 3 - \epsilon$, the first two terms in Eq. (68) are the leading contribution, and $H(\zeta)$ corresponds to higher-order terms.

Now, adding all contributions together, the layer susceptibility of the transverse mode is

$$\begin{aligned}
\chi^T(z_1, z_2) = & \chi_0^T(z_1, z_2) + 36b'_{11} + 12N b'_{12} + 24\tilde{b}'_2 + 576b'_{23} \\
= & \frac{1}{2} \sqrt{z_1 z_2} \zeta - \left(\frac{3(d+1)}{5-d} + N + \frac{15\left(\frac{d+1}{5-d} + \frac{N-1}{5}\right)}{(d-4)d} \right) \frac{\gamma_T}{8} \sqrt{\frac{u_0}{10}} (z_1 z_2)^{\frac{4-d}{2}} \left(A \zeta^{\frac{5-d}{2}} + B \zeta^{\frac{d-1}{2}} \right) \\
& + \frac{3}{32} \frac{S_{d-1}}{(2\pi)^{d-1}} \sqrt{\frac{u_0}{10}} (z_1 z_2)^{\frac{4-d}{2}} \left(A C_1 \zeta^{\frac{5-d}{2}} + B C_2 \zeta^{\frac{d-1}{2}} \right) + 576 (z_1 z_2)^{\frac{4-d}{2}} H(\zeta). \tag{71}
\end{aligned}$$

3.3 Layer susceptibility of the longitudinal mode

We consider the two-point functions of the longitudinal mode $\langle \phi_1(z) \phi_1(z') \rangle$ with the one-loop Feynman diagrams shown in Fig 3. Using the same method as in Sec. 3.2, we can calculate the diagrams straightforwardly. The symmetry factor of c_{11} and c_{12} in Fig. 3 (a), are, respectively, 180 and $36(N-1)$. We can directly calculate the corresponding layer susceptibility

$$\begin{aligned}
c'_{11} = & \frac{-u_0}{6!} \int dy (m_0(y))^2 G_0^L(0, y, y) \chi_0^L(z_1, y) \chi_0^L(z_2, y) = -\frac{\gamma_L \sqrt{\frac{u_0}{10}}}{384} (z_1 z_2)^{\frac{4-d}{2}} \left(A' \zeta^{\frac{d+1}{2}} + B' \zeta^{\frac{7-d}{2}} \right), \\
c'_{12} = & \frac{-u_0}{6!} \int dy (m_0(y))^2 G_0^T(0, y, y) \chi_0^L(z_1, y) \chi_0^L(z_2, y) = -\frac{\gamma_T \sqrt{\frac{u_0}{10}}}{384} (z_1 z_2)^{\frac{4-d}{2}} \left(A' \zeta^{\frac{d+1}{2}} + B' \zeta^{\frac{7-d}{2}} \right), \tag{72}
\end{aligned}$$

where we used the mean-field quantities in Eqs. (46), (48), (47) and performed the integration. Here $\zeta = \frac{\min(z_1, z_2)}{\max(z_1, z_2)}$, $A' = \frac{-4}{(d-3)(d+1)}$ and $B' = \frac{-4}{(d-7)(d-3)}$.

Next, we calculate the two-vertex diagrams shown in Fig. 3 (b). The combination of c_{21} and c_{22} can be expressed again with the help of m_1 in Fig. 1. Hence, we define such a combination as \tilde{c}_2 . We have the symmetry factors 120, 7776 and $288(N-1)$ for \tilde{c}_2 , c_{23} and c_{24} , respectively, leading to the higher-order correction: $120\tilde{c}_2 + 7776c_{23} + 288(N-1)c_{24}$.

We will evaluate the layer susceptibility corresponding to \tilde{c}_2 , c_{23} and c_{24} in the following. The calculation for \tilde{c}_2 is straightforward:

$$\begin{aligned} \tilde{c}'_2 &= \frac{-u_0}{6!} \int dy (m_0(y))^3 \chi_0^L(z_1, y) \chi_0^L(z_2, y) m_1(y) \\ &= -\frac{\gamma_T \sqrt{\frac{5u_0}{2} \left(\frac{d+1}{5-d} + \frac{N-1}{5} \right)}}{256(d-4)d} (z_1 z_2)^{\frac{4-d}{2}} \left(A' \zeta^{\frac{d+1}{2}} + B' \zeta^{\frac{7-d}{2}} \right), \end{aligned} \quad (73)$$

where to get the second line, a similar integration has been performed.

The evaluations for diagrams c_{23} and c_{24} are similar, so we present them together. The corresponding layer susceptibilities are

$$\begin{aligned} c'_{23} &= \left(\frac{-u_0}{6!} \right)^2 \int dy_1 dy_2 \chi_0^L(z_1, y_1) \chi_0^L(z_2, y_2) (m_0(y_1))^3 (m_0(y_2))^3 B^{LL}(y_1, y_2), \\ c'_{24} &= \left(\frac{-u_0}{6!} \right)^2 \int dy_1 dy_2 \chi_0^L(z_1, y_1) \chi_0^L(z_2, y_2) (m_0(y_1))^3 (m_0(y_2))^3 B^{TT}(y_1, y_2), \end{aligned} \quad (74)$$

where $B^{LL}(y_1, y_2) = \int d^{d-1} r (G_0^L(r, y_1, y_2))^2$ and $B^{TT}(y_1, y_2) = \int d^{d-1} r (G_0^T(r, y_1, y_2))^2$. Via a similar Fourier transformation in the parallel hyperspace, we can arrive at

$$\begin{aligned} B^{LL}(y_1, y_2) &= \frac{S_{d-1}}{(2\pi)^{d-1}} y_1 y_2 \int dp p^{d-2} I_2(p y_1) K_2(p y_2) I_2(p y_1) K_2(p y_2) \\ &= \frac{S_{d-1}}{(2\pi)^{d-1}} \frac{1}{4} y_1^{3-d} \left(\frac{y_1}{y_2} \right)^{2+d} \Gamma\left(\frac{5}{2}\right) \Gamma\left(\frac{d-1}{2}\right) \Gamma\left(\frac{d+3}{2}\right) \Gamma\left(\frac{d+7}{2}\right) \\ &\quad \times {}_4\tilde{F}_3\left[\left\{\frac{5}{2}, \frac{d-1}{2}, \frac{d+3}{2}, \frac{d+7}{2}\right\}, \left\{3, 5, \frac{d+4}{2}\right\}, \left(\frac{y_1}{y_2}\right)^2\right], \\ B^{TT}(y_1, y_2) &= \frac{S_{d-1}}{(2\pi)^{d-1}} y_1 y_2 \int dp p^{d-2} I_1(p y_1) K_1(p y_2) I_1(p y_1) K_1(p y_2) \\ &= \frac{S_{d-1}}{(2\pi)^{d-1}} \frac{1}{4} y_1^{3-d} \left(\frac{y_1}{y_2} \right)^d \Gamma\left(\frac{3}{2}\right) \Gamma\left(\frac{d-1}{2}\right) \Gamma\left(\frac{d+1}{2}\right) \Gamma\left(\frac{d+3}{2}\right) \\ &\quad \times {}_4\tilde{F}_3\left[\left\{\frac{3}{2}, \frac{d-1}{2}, \frac{d+1}{2}, \frac{d+3}{2}\right\}, \left\{2, 3, \frac{d+2}{2}\right\}, \left(\frac{y_1}{y_2}\right)^2\right]. \end{aligned} \quad (75)$$

where we have assumed $y_1 < y_2$. The result for $y_1 > y_2$ can be obtained by exchanging y_1

and y_2 . Hence, c'_{23} and c'_{24} can be evaluated as follows,

$$\begin{aligned}
c'_{23} &= \left(\frac{-u_0}{6!}\right)^2 \left(\frac{90}{u_0}\right)^{\frac{3}{2}} \frac{1}{16} \sqrt{z_1 z_2} \left(\int_0^\infty dy_1 \int_{y_1}^\infty dy_2 + \int_0^\infty dy_2 \int_{y_2}^\infty dy_1 \right) \frac{1}{y_1 y_2} \\
&\quad \times \left(\frac{\min(z_1, y_1)}{\max(z_1, y_1)} \right)^2 \left(\frac{\min(z_2, y_2)}{\max(z_2, y_2)} \right)^2 B^{LL}(\min(y_1, y_2), \max(y_1, y_2)) \\
&\equiv \left(\frac{-u_0}{6!}\right)^2 \left(\frac{90}{u_0}\right)^{\frac{3}{2}} \frac{1}{16} \sqrt{z_1 z_2} \frac{S_{d-1}}{(2\pi)^{d-1}} \frac{1}{4} \Gamma\left(\frac{5}{2}\right) \Gamma\left(\frac{d-1}{2}\right) \Gamma\left(\frac{d+3}{2}\right) \Gamma\left(\frac{d+7}{2}\right) (I'_1 + I'_2), \\
c'_{24} &= \left(\frac{-u_0}{6!}\right)^2 \left(\frac{90}{u_0}\right)^{\frac{3}{2}} \frac{1}{16} \sqrt{z_1 z_2} \left(\int_0^\infty dy_1 \int_{y_1}^\infty dy_2 + \int_0^\infty dy_2 \int_{y_2}^\infty dy_1 \right) \frac{1}{y_1 y_2} \\
&\quad \times \left(\frac{\min(z_1, y_1)}{\max(z_1, y_1)} \right)^2 \left(\frac{\min(z_2, y_2)}{\max(z_2, y_2)} \right)^2 B^{TT}(\min(y_1, y_2), \max(y_1, y_2)) \\
&\equiv \left(\frac{-u_0}{6!}\right)^2 \left(\frac{90}{u_0}\right)^{\frac{3}{2}} \frac{1}{16} \sqrt{z_1 z_2} \frac{S_{d-1}}{(2\pi)^{d-1}} \frac{1}{4} \Gamma\left(\frac{3}{2}\right) \Gamma\left(\frac{d-1}{2}\right) \Gamma\left(\frac{d+1}{2}\right) \Gamma\left(\frac{d+3}{2}\right) (I''_1 + I''_2),
\end{aligned} \tag{76}$$

where $I'_{1,2}$ and $I''_{1,2}$ are integrals detailed in Appendix B.3. The details of the evaluation for integrals I'_1 and I'_2 can be found in Appendix B.3. The final result for c'_{23} is

$$c'_{23} = \frac{90^{\frac{3}{2}}}{(6!)^2} \frac{S_{d-1}}{128(2\pi)^{d-1}} \sqrt{u_0} (z_1 z_2)^{\frac{4-d}{2}} \left(A' C'_1 \zeta^{\frac{d+1}{2}} + B' C'_2 \zeta^{\frac{7-d}{2}} \right) + (z_1 z_2)^{\frac{4-d}{2}} H'(\zeta), \tag{77}$$

where C'_1 and C'_2 are given explicitly in Appendix B.3. Their numerical values up to $\mathcal{O}(\epsilon)$ are

$$C'_1 = \frac{16}{15} + c'_{1,1} \epsilon + \mathcal{O}(\epsilon^2), \quad C'_2 = \frac{16}{15} + c'_{2,1} \epsilon + \mathcal{O}(\epsilon^2), \tag{78}$$

with $c'_{1,1} \approx -1.45699$ and $c'_{2,1} \approx -1.35775$. And the last term in c'_{23} is

$$\begin{aligned}
H'(\zeta) &= \frac{90^{\frac{3}{2}}}{(6!)^2} \frac{S_{d-1}}{128(2\pi)^{d-1}} \Gamma\left(\frac{5}{2}\right) \Gamma\left(\frac{d-1}{2}\right) \Gamma\left(\frac{d+3}{2}\right) \Gamma\left(\frac{d+7}{2}\right) \sqrt{u_0} \zeta^{\frac{d+7}{2}} \\
&\quad \left\{ A' \Gamma\left(\frac{d+4}{2}\right) {}_5\tilde{F}_4 \left[\left\{ \frac{d+4}{2}, \frac{5}{2}, \frac{d-1}{2}, \frac{d+3}{2}, \frac{d+7}{2} \right\}, \left\{ \frac{d+6}{2}, 3, 5, \frac{d+4}{2} \right\}, \zeta^2 \right] \right. \\
&\quad - A' \Gamma\left(\frac{3}{2}\right) {}_5\tilde{F}_4 \left[\left\{ \frac{3}{2}, \frac{5}{2}, \frac{d-1}{2}, \frac{d+3}{2}, \frac{d+7}{2} \right\}, \left\{ \frac{5}{2}, 3, 5, \frac{d+4}{2} \right\}, \zeta^2 \right] \\
&\quad + B' \Gamma\left(\frac{7}{2}\right) {}_5\tilde{F}_4 \left[\left\{ \frac{7}{2}, \frac{5}{2}, \frac{d-1}{2}, \frac{d+3}{2}, \frac{d+7}{2} \right\}, \left\{ \frac{9}{2}, 3, 5, \frac{d+4}{2} \right\}, \zeta^2 \right] \\
&\quad \left. - B' \Gamma\left(\frac{d}{2}\right) {}_5\tilde{F}_4 \left[\left\{ \frac{d}{2}, \frac{5}{2}, \frac{d-1}{2}, \frac{d+3}{2}, \frac{d+7}{2} \right\}, \left\{ \frac{d+2}{2}, 3, 5, \frac{d+4}{2} \right\}, \zeta^2 \right] \right\}.
\end{aligned} \tag{79}$$

Similarly, we can get c'_{24}

$$c'_{24} = \frac{90^{\frac{3}{2}}}{(6!)^2} \frac{S_{d-1}}{128(2\pi)^{d-1}} \sqrt{u_0} (z_1 z_2)^{\frac{4-d}{2}} \left(A' C''_1 \zeta^{\frac{d+1}{2}} + B' C''_2 \zeta^{\frac{7-d}{2}} \right) + (z_1 z_2)^{\frac{4-d}{2}} H''(\zeta), \tag{80}$$

where

$$\begin{aligned}
C''_1 &= \frac{8}{3} + c''_{1,1} \epsilon + \mathcal{O}(\epsilon^2), \quad C''_2 = \frac{8}{3} + c''_{2,1} \epsilon + \mathcal{O}(\epsilon^2), \\
c''_{1,1} &\approx -1.64248, \quad c''_{2,1} \approx -0.263237.
\end{aligned} \tag{81}$$

and

$$\begin{aligned}
H''(\zeta) = & \frac{90^{\frac{3}{2}}}{(6!)^2} \frac{S_{d-1}}{128(2\pi)^{d-1}} \Gamma\left(\frac{3}{2}\right) \Gamma\left(\frac{d-1}{2}\right) \Gamma\left(\frac{d+1}{2}\right) \Gamma\left(\frac{d+3}{2}\right) \sqrt{u_0} \zeta^{\frac{d+3}{2}} \\
& \left\{ A' \Gamma\left(\frac{d+2}{2}\right) {}_5\tilde{F}_4 \left[\left\{ \frac{d+2}{2}, \frac{3}{2}, \frac{d-1}{2}, \frac{d+1}{2}, \frac{d+3}{2} \right\}, \left\{ \frac{d+4}{2}, 2, 3, \frac{d+2}{2} \right\}, \zeta^2 \right] \right. \\
& - A' \Gamma\left(\frac{1}{2}\right) {}_5\tilde{F}_4 \left[\left\{ \frac{1}{2}, \frac{3}{2}, \frac{d-1}{2}, \frac{d+1}{2}, \frac{d+3}{2} \right\}, \left\{ \frac{3}{2}, 2, 3, \frac{d+2}{2} \right\}, \zeta^2 \right] \\
& + B' \Gamma\left(\frac{5}{2}\right) {}_5\tilde{F}_4 \left[\left\{ \frac{5}{2}, \frac{3}{2}, \frac{d-1}{2}, \frac{d+1}{2}, \frac{d+3}{2} \right\}, \left\{ \frac{7}{2}, 2, 3, \frac{d+2}{2} \right\}, \zeta^2 \right] \\
& \left. - B' \Gamma\left(\frac{d-2}{2}\right) {}_5\tilde{F}_4 \left[\left\{ \frac{d-2}{2}, \frac{3}{2}, \frac{d-1}{2}, \frac{d+1}{2}, \frac{d+3}{2} \right\}, \left\{ \frac{d}{2}, 2, 3, \frac{d+2}{2} \right\}, \zeta^2 \right] \right\}. \tag{82}
\end{aligned}$$

The explicit expression for $C''_{1,2}$ can be found in Appendix B.3. It is obvious that for $d = 3 - \epsilon$, the first two terms in c'_{23} and c'_{24} are the leading contribution, while $H'(\zeta)$ and $H''(\zeta)$ correspond to higher-order terms.

Totally, we can sum over all Feynman diagrams and get the layer susceptibility for $\chi^L(z_1, z_2)$ that

$$\begin{aligned}
\chi^L(z_1, z_2) = & \chi_0^L + 180c'_{11} + 36(N-1)c'_{12} + 120(c_{21} + c_{22})' + 7776c'_{23} + 288(N-1)c'_{24} \\
= & \frac{1}{4} \sqrt{z_1 z_2} \zeta^2 - \left(\frac{15(d+1)}{5-d} + 3(N-1) + \frac{75\left(\frac{d+1}{5-d} + \frac{N-1}{5}\right)}{(d-4)d} \right) \frac{\gamma_T}{32} \sqrt{\frac{u_0}{10}} (z_1 z_2)^{\frac{4-d}{2}} \left(A' \zeta^{\frac{d+1}{2}} + B' \zeta^{\frac{7-d}{2}} \right) \\
& + \frac{3}{256} \frac{S_{d-1}}{(2\pi)^{d-1}} \sqrt{\frac{u_0}{10}} (z_1 z_2)^{\frac{4-d}{2}} \left(A' [27C'_1 + (N-1)C''_1] \zeta^{\frac{d+1}{2}} + B' [27C'_2 + (N-1)C''_2] \zeta^{\frac{7-d}{2}} \right) \\
& + 7776(z_1 z_2)^{\frac{4-d}{2}} H'(\zeta) + 288(N-1)(z_1 z_2)^{\frac{4-d}{2}} H''(\zeta). \tag{83}
\end{aligned}$$

4 Boundary operator expansion

Now we consider the boundary operator expansion (BOE). With the results in section 3, we can express the layer susceptibility as a power of $\zeta = \frac{\min(z, z')}{\max(z, z')}$. The corresponding prefactor will give us the boundary operator expansion coefficients [11], as shown in Eq. (1) and (5).

4.1 BOE of the transverse mode

As in Eq. (5), the layer susceptibility $\chi^T(z_1, z_2)$ can be expanded in the following form

$$\chi^T(z_1, z_2) = \sqrt{4z_1 z_2} \zeta^{-\frac{d-1}{2}} \left(c_{d-1}^T \zeta^{d-1} + \sum_{\Delta > d-1} c_{\Delta}^T \zeta^{\Delta} \right). \tag{84}$$

From the one-loop result in Eq. (71), the leading order result gives

$$c_{d-1}^T = \frac{1}{4} - \frac{2 + 3c_{1,1} - 3c_{2,1}}{128\pi} \sqrt{\frac{u_0}{10}} = \frac{1}{4} - \frac{2 + 3c_{1,1} - 3c_{2,1}}{16} \sqrt{\frac{3}{2(3N+22)}} \epsilon^{\frac{1}{2}} + \mathcal{O}(\epsilon^{\frac{3}{2}}), \tag{85}$$

where in the first equality, we have taken $d = 3$ while kept the u_0 coupling. The appearance of seemingly $\mathcal{O}(\epsilon)$ contributions $c_{1,1}$ and $c_{2,1}$ is because of the leading $\mathcal{O}(1/\epsilon)$ contribution in the constants A and B . In the last expression, we substituted $u_0 = Z_u u$ with the fixed point value in Eq. (51). We expect that the appearance of the field with scaling dimension of $d-1$ at both

the leading and subleading order is related to the broken $O(N)$ symmetry at the boundary. It would be interesting to investigate the Ward identity associated with the $O(N)$ current and demonstrate this explicitly.

The higher-order terms in BOE come from $H_d(\zeta)$. We use the expansion of the regularized generalized hypergeometric function:

$${}_5\tilde{F}_4[\{a_1, \dots, a_5\}, \{b_1, \dots, b_4\}, z] = \sum_{k=0}^{\infty} \frac{\frac{\Gamma(a_1+k)}{\Gamma(a_1)} \frac{\Gamma(a_2+k)}{\Gamma(a_2)} \frac{\Gamma(a_3+k)}{\Gamma(a_3)} \frac{\Gamma(a_4+k)}{\Gamma(a_4)} \frac{\Gamma(a_5+k)}{\Gamma(a_5)}}{\Gamma(k+1)\Gamma(b_1+k)\Gamma(b_2+k)\Gamma(b_3+k)\Gamma(b_4+k)} z^k. \quad (86)$$

With this expansion, $H(\zeta)$ can be rewritten as a series

$$H(\zeta) = \frac{90^{\frac{3}{2}}}{(6!)^2} \frac{S_{d-1}}{32(2\pi)^{d-1}} \sqrt{u_0} \zeta^{\frac{d+5}{2}} \sum_{k=0}^{\infty} \frac{\Gamma(\frac{d-1}{2}+k)\Gamma(\frac{5}{2}+k)\Gamma(\frac{d+1}{2}+k)\Gamma(\frac{d+5}{2}+k)}{\Gamma(k+1)\Gamma(3+k)\Gamma(\frac{d+2}{2}+k)\Gamma(4+k)} \left(\frac{A}{\frac{5}{2}+k} - \frac{A}{\frac{d}{2}+k} + \frac{B}{\frac{d+2}{2}+k} - \frac{B}{\frac{3}{2}+k} \right) \zeta^{2k}. \quad (87)$$

Substitute this expansion to the layer susceptibility and compare it with the coefficient defined in Eq. (84), we arrive at

$$c_k^T = \frac{3}{8\pi} \frac{1}{k^2(k-1)(k-2)^2} \sqrt{\frac{u_0}{10}} = \frac{3}{2} \sqrt{\frac{6}{3N+22}} \frac{1}{k^2(k-1)(k-2)^2} \epsilon^{\frac{1}{2}}, \quad k = 5, 7, 9, \dots \quad (88)$$

Note that in the first equality, we have taken $d = 3$ while kept u_0 . In the last expression, we have further set u_0 to be the fixed point value.

There are three additional remarks. i) It is worth noting that in contrast to the ϕ^4 theory, the leading term in the ϵ expansion is $\mathcal{O}(\epsilon^{1/2})$. This is not a coincidence because the power of $\mathcal{O}(\epsilon^{1/2})$ also appears at the special transition [54]. ii) Naively, setting $\epsilon = 0$ in the final expression of c_k^T for $d = 3$ seems to indicate that BOE vanishes at the leading order. However, in strictly $d = 3$, u_0 is given by a logarithmic flow, $u_0 \sim \frac{1}{\log \mu_0 z}$. Substituting this logarithmic flow to the expression of BOE with explicit u_0 dependence reveals that BOE has a logarithmic dependence instead of being completely trivial. iii) In general, with c_k^T in Eq. (1), we can reconstruct the Green's function $G^T(\xi, z_1, z_2)$ by resumming the finite series. While this can be done explicitly for the critical $O(N)$ model with $N = 2$ [11], we are not able to get a compact form for the tricritical point. But we can get the expansion of $G^T(\xi, z_1, z_2)$ as a series of ξ^n with known prefactors.⁵

4.2 BOE of the longitudinal mode

The BOE for the longitudinal mode can be obtained similarly. The layer susceptibility $\chi^L(z_1, z_2)$ can be expanded in the following form

$$\chi^L(z_1, z_2) = \sqrt{4z_1 z_2} \zeta^{-\frac{d-1}{2}} \left(c_d^L \zeta^d + \sum_{\Delta > d} c_{\Delta}^L \zeta^{\Delta} \right). \quad (89)$$

We can simplify the first two lines in the last equality in Eq. (83), with all known constants γ_T, A', B' , and $C'_{1,2}, C''_{1,2}$. A further simplification is done by setting $d = 3$. The simplification

⁵We can express ${}_2\tilde{F}_1$ with the integration representation, expand with respect to ξ and do the integral to get the prefactor of ξ^n .

is straightforward, so we skip the derivation. The final result gives the leading coefficient,

$$\begin{aligned} c_d^L &= \frac{1}{8} + \frac{16 + 405(c'_{1,1} - c'_{2,1}) + 15(N-1)(c''_{1,1} - c''_{2,1})}{640} \frac{1}{8\pi} \sqrt{\frac{u_0}{10}} \\ &= \frac{1}{8} + \frac{16 + 405(c'_{1,1} - c'_{2,1}) + 15(N-1)(c''_{1,1} - c''_{2,1})}{640} \sqrt{\frac{3}{2(3N+22)}} \epsilon^{\frac{1}{2}} + \mathcal{O}(\epsilon). \end{aligned} \quad (90)$$

This operator with scaling dimension d is the displacement operator. The presence of a boundary breaks the translation symmetry. As a result, the conservation of stress-energy tensor is violated by a boundary term, the displacement operator. Hence, its scaling dimension is projected to be d .

$H'(\zeta)$ and $H''(\zeta)$ contribute to the higher order coefficients. Using the same formula Eq. (86) and after some tedious manipulation not shown here, we can get the higher order expansions for the leading order in ϵ expansion,

$$\begin{aligned} \sum_{\Delta} c_{\Delta}^L \zeta^{\Delta} &= \frac{3}{1024\pi} \sqrt{\frac{u_0}{10}} \\ &\times \left[27 \sum_{k=0}^{\infty} \frac{1}{k + \frac{5}{2}} \frac{32}{(21 + 20k + 4k^2)^2} \zeta^{2k+6} + (N-1) \sum_{k=0}^{\infty} \frac{1}{k + \frac{3}{2}} \frac{32}{(5 + 12k + 4k^2)^2} \zeta^{2k+4} \right]. \end{aligned} \quad (91)$$

Therefore, we have the prefactor,

$$\begin{aligned} c_4^L &= \frac{3}{16\pi} \frac{N-1}{(k-3)^2(k-1)(k+1)^2} \sqrt{\frac{u_0}{10}} \\ &= \frac{3}{2} \sqrt{\frac{3}{2(3N+22)}} \cdot \frac{N-1}{(k-3)^2(k-1)(k+1)^2} \epsilon^{\frac{1}{2}} + \mathcal{O}(\epsilon), \\ c_k^L &= \frac{3}{16\pi} \frac{N+26}{(k-3)^2(k-1)(k+1)^2} \sqrt{\frac{u_0}{10}} \\ &= \frac{3}{2} \sqrt{\frac{3}{2(3N+22)}} \cdot \frac{N+26}{(k-3)^2(k-1)(k+1)^2} \epsilon^{\frac{1}{2}} + \mathcal{O}(\epsilon), \quad k = 6, 8, 10, \dots \end{aligned} \quad (92)$$

Again, we see the leading term in the ϵ expansion is $\mathcal{O}(\epsilon^{1/2})$. We also keep the expression with u_0 in the first equality, such that in strictly $d = 3$, u_0 is given by a logarithmic flow, $u_0 \sim \frac{1}{\log \mu_0 z}$.

5 Extraordinary phase in tricritical $O(N)$ model

We first briefly review the extraordinary-log transition in the critical $O(N)$ model described in Ref. [16], and then consider the situation of the tricritical $O(N)$ model.

5.1 IR description of the extraordinary-log transition

To investigate the extraordinary-log transition, we imagine stripping away the outermost boundary layer of the system. Then the system without the outermost layer is described by the ordinary transition. On the other hand, because we are interested in the extraordinary transition, the order parameter is ordered in the outermost layer. It can be modeled by a nonlinear sigma model [57, 58] with $g \sim 0$. We, then, couple the ordinary transition action to the nonlinear sigma model according to $O(N)$ symmetry. This is the UV description of the extraordinary-log transition [16]:

$$S_{UV} = S_{\text{ordinary}} + S_n + S_{n\phi}. \quad (93)$$

where S_{ordinary} denotes the bulk action at the ordinary transition. Here, S_n is the nonlinear sigma model and $S_{n\phi}$ describes the coupling between the bulk and the outermost layer, given by

$$S_n = \int d^{d-1}r \frac{1}{2g} (\partial_\mu \vec{n})^2, \quad S_{n\phi} = -s' \int d^{d-1}r \vec{n}(x) \cdot \vec{\phi}(x). \quad (94)$$

where $\vec{\phi}$ is the bulk $O(N)$ field and s' is the coupling between the bulk and boundary fields.⁶ Notice that for the nonlinear sigma model, we have $g \sim 0$ and $\vec{n}^2 = 1$. Without loss of generality, we take $n_1 = 1$ and $n_i = 0$ for $i > 1$ to be the ordered direction.

Because \vec{n} is ordered, we expect that the bulk action will flow to the normal boundary condition. The normal boundary condition is actually equivalent to the extraordinary transition. We describe the bulk-boundary OPE for the normal boundary condition for later convenience. The bulk-boundary OPE of the critical $O(N)$ field reads,

$$\phi_1(r, z) \sim \frac{a_\sigma}{(2z)^{\Delta_\phi}} + \frac{a'_\sigma}{(2z)^{\Delta_\phi - d}} \hat{D} + \dots, \quad (95a)$$

$$\phi_i(r, z) \sim \frac{b_t}{(2z)^{\Delta_\phi - (d-1)}} \hat{t}_i + \dots, \quad i > 1. \quad (95b)$$

In the expansion of the longitudinal component, ϕ_1 , a_σ is the normalization of the single point function, and \hat{D} is the displacement operator with scaling dimension d . In the expansion of the transverse component, ϕ_i , $i > 1$, \hat{t}_i is the ‘‘tilt’’ field, which is the $O(N-1)$ vector with the lowest scaling dimension, $d-1$.

Including the coupling with the nonlinear sigma model, the IR description of the extraordinary is

$$S_{\text{IR}} = S_{\text{normal}} + S_n - s \int d^{d-1}r \sum_{i>1} \pi_i(r) \hat{t}_i(r) + \delta S, \quad (96)$$

where δS corresponds to the irrelevant terms and $\vec{n} = (\sqrt{1 - \vec{\pi}^2}, \vec{\pi})$. s is the IR coupling between the bulk and boundary field, and crucially, it is fixed by the $O(N)$ symmetry [16].

While the $O(N)$ symmetry is not explicit in Eq. (96), the theory should respect $O(N)$ symmetry. Now consider a small rotation of the ordered direction. For instance, consider a rotation from the first component (which is assumed to be ordered) to the second component by an angle α . It leads to a nonvanishing one-point function for the second component,

$$\langle \phi_2(0, z) \rangle = \sin \alpha \frac{a_\sigma}{(2z)^{\Delta_\phi}} \approx \alpha \frac{a_\sigma}{(2z)^{\Delta_\phi}}. \quad (97)$$

Due to the $O(N)$ symmetry, such a result should also be obtained from the IR theory Eq. (96). Because $\vec{n} = (\cos \alpha, \sin \alpha, 0, \dots)$ after the rotation, the second component of the $O(N)$ field, ϕ_2 , has a nonvanishing expectation value as expected. We calculate this expectation value using the IR theory at the leading order,

$$\langle \phi_2(0, z) \rangle \approx \alpha s \int d^{d-1}r \langle \phi_2(0, z) \hat{t}_2(r) \rangle_{\text{normal}} \quad (98)$$

$$= \alpha s \int d^{d-1}r \frac{b_t (2z)^{d-1-\Delta_\phi}}{(r^2 + z^2)^{d-1}} = \alpha s b_t \frac{(4\pi)^{\frac{d-1}{2}} \Gamma(\frac{d-1}{2})}{\Gamma(d-1)} \frac{1}{(2z)^{\Delta_\phi}}. \quad (99)$$

Equating this to Eq. (97), we can fix the value of s [16],

$$s = \frac{\Gamma(d-1)}{(4\pi)^{\frac{d-1}{2}} \Gamma(\frac{d-1}{2})} \frac{a_\sigma}{b_t}. \quad (100)$$

⁶ s' is different from s in the IR theory.

Note that this value is fixed by the $O(N)$ symmetry, and does not flow under RG.

After fixing the coupling between the bulk and boundary fields, we are at the position to look at the effect of such a coupling to the RG equation of the nonlinear sigma model. The lowest order RG can be obtained straightforwardly [16],

$$\frac{dg}{d \log \mu} = \beta_g, \quad \beta_g = -\frac{N-2}{2\pi} g^2 + \frac{\pi s^2}{2} g^2, \quad (101)$$

where $\frac{N-2}{2\pi} g^2$ is the well-known result from the conventional nonlinear sigma model, while the second term is from the coupling to the bulk field.

In the conventional nonlinear sigma model, $N > 2$ the system flows to a strongly coupled fixed point at IR that restores the symmetry, presenting a short-range correlated state. When $N = 2$, the one-loop RG equation vanishes, and the system is essentially described by a quasi-long range order. This is the seminal result of the Mermin–Wagner theorem. The presence of the second term can reverse the RG flow to a weakly coupled fixed point, $g \sim 0$, when $N < N_c$ with

$$N_c = 2 + \pi^2 s^2. \quad (102)$$

The logarithmic flow to this weakly coupled fixed point leads to a logarithmic correlation of the boundary field. One should notice that the one-point function also decays logarithmically, indicating that no true long-range order has developed. Because $a_\sigma, b_t > 0$, the above analysis implies $N_c > 2$. A conformal bootstrap study of the normal fixed point showed that $N_c > 3$ [59] for the critical $O(N)$ model.

5.2 Extraordinary transition at the tricritical point

The above analysis reveals that the RG invariant quantity s crucially determines the critical flavor. As s is fixed by the bulk-boundary OPE of the $O(N)$ field, we can obtain this via the BOE of layer susceptibility.

Firstly, recall that the order parameter profile $m(z)$ is precisely the one-point function of the longitudinal component. Hence, at the one-loop level, a_σ is given by Eq. (59). Next, we extract b_t from the BOE of the two-point function. According to the BOE of layer susceptibility listed in Sec. 4.1, the BOE of two-point function reads,

$$\begin{aligned} G^T(r, z, z') &= (4zz')^{-\Delta_\phi} c_{d-1} \sigma_{d-1} \mathcal{G}_{\text{boe}}(d-1, \xi) + \dots \\ &= (4zz')^{-\Delta_\phi} c_{d-1}^T \sigma_{d-1} \xi^{d-1} + \dots, \quad \xi \rightarrow \infty. \end{aligned} \quad (103)$$

where in the second line a boundary limit have been taken $\xi \rightarrow \infty$. Compared this with the bulk-boundary OPE in Eq. (95b), we arrive at

$$b_t^2 = c_{d-1}^T \sigma_{d-1} = \frac{1}{16\pi} - \frac{2 + 3c_{1,1} - 3c_{2,1}}{64\pi} \sqrt{\frac{3}{2(3N+22)}} \epsilon^{\frac{1}{2}} + \mathcal{O}(\epsilon). \quad (104)$$

Hence, we can calculate s from Eq. (100) for the tricritical point:

$$s^2 = \frac{1}{2\pi^2} \sqrt{\frac{3(3N+22)}{2}} \epsilon^{-\frac{1}{2}} + \frac{78 + 8N + 9c_{1,1} - 9c_{2,1}}{16\pi^2} + \mathcal{O}(\epsilon^{\frac{1}{2}}). \quad (105)$$

The critical flavor is given by

$$N_c = 2 + \sqrt{\frac{3(3N+22)}{8}} \epsilon^{-\frac{1}{4}}, \quad (106)$$

which increases as ϵ decreases. Naively, it implies that the critical flavor for the tricritical $O(N)$ model in three dimensions is infinity, i.e., extraordinary-log transition exists for all flavors, $N \geq 2$. However, when $\epsilon = 0$, the bulk coupling constant u exhibits a logarithmic flow, which affects the BOE as we have seen in the previous section. Hence, we should incorporate the RG equations for both s and g . To this end, considering the coupling s given in Eq. (100), and the logarithmic flow of BOE coefficient a_σ discussed below Eq. (59), we can get the following coupled RG equations:

$$\frac{ds}{d \log \mu} = -\frac{3(3N+22)}{128\pi^4} s^{-3}, \quad (107)$$

$$\frac{dg}{d \log \mu} = -\frac{N-2}{2\pi} g^2 + \frac{\pi s^2}{2} g^2. \quad (108)$$

The solution in the long-wave length limit is ⁷

$$s \approx \left[\frac{3(3N+22)}{2(2\pi)^4} \log \mu_0 l \right]^{1/4}, \quad g \approx \frac{48(N-2)\pi}{3N+22} (\log \mu_0 l)^{-2} + \sqrt{\frac{96\pi^2}{3N+22}} (\log \mu_0 l)^{-3/2}. \quad (109)$$

where μ_0 is an arbitrary energy scale, and l denotes the length scale of the system. The IR limit corresponds to the long wavelength, $l \rightarrow \infty$. It is important to note that the product sg flows to zero at IR, which justifies the perturbative calculation. Namely, the RG calculation in Eq. (101) has used a perturbation of sg , which is obvious from the second term of the beta function.

Now we can solve the Callan-Symanzyk equation for the renormalized correlation,

$$D_r^m = Z_n^{-m/2} \langle n(x_1) \dots n(x_m) \rangle, \quad (110)$$

where Z_n is the RG factor for n , and satisfies the equation [16]

$$\mu \frac{\partial}{\partial \mu} \log Z_n = \eta(g), \quad \eta(g) = \frac{N-1}{2\pi} g. \quad (111)$$

The Callan-Symanzyk equation is given by

$$\left(\mu \frac{\partial}{\partial \mu} + \beta(g) \frac{\partial}{\partial g} + \frac{m}{2} \eta(g) \right) D_r^m(g, \mu) = 0. \quad (112)$$

Here, the beta equation β_g involves a logarithmic flow of the bulk-boundary coupling s , in contrast to the critical $O(N)$ model in which the bulk-boundary coupling is a constant. Thus, we have the following Callan-Symanzyk equation

$$\left(\mu \frac{\partial}{\partial \mu} + \left(\frac{\pi}{2} \sqrt{\frac{3(3N+22)}{2(2\pi)^4}} \log \mu - \frac{N-2}{2\pi} \right) g^2 \frac{\partial}{\partial g} + \frac{m}{2} \frac{N-1}{2\pi} g \right) D_r^m = 0. \quad (113)$$

From the Callan-Symanzyk equation, we can get the expectation value of the surface order,

$$\langle n \rangle_r \sim \exp \left[(N-1) \sqrt{\frac{24}{3N+22}} \left(\log \frac{\mu_0}{\sqrt{h}} \right)^{-1/2} \right], \quad h \rightarrow 0, \quad (114)$$

where h represents an external field linearly coupled to the surface order \vec{n} , while μ_0 is an arbitrary energy scale. We can see that as the external field h decreases to zero, the expectation

⁷The full solution is given in Appendix C

of the surface order does not vanish! Also, the correlation function is dominated by the finite orders in this case,

$$\langle n(x)n(0) \rangle_r \sim \exp \left[4(N-1) \sqrt{\frac{6}{3N+22}} (\log \mu_0 x)^{-1/2} \right], \quad x \gg 1. \quad (115)$$

On top of the ordered configuration, we expect the correlation will be given by the leading boundary primary field, namely, the displacement field in the longitudinal mode and the tilt field in the transverse mode.

It is illuminating to give a general discussion about the logarithmic flow of the coupling constant g and the surface order. While the coupling constant g flows to zero logarithmically in both the extraordinary-log phase in the critical $O(N)$ model and the extraordinary phase tricritical point discussed above, whether the surface order parameter is vanishing or not actually depends on the form of the log flow. Consider a general log flow in the long-wavelength $\mu \ll \mu_0$ of the form

$$g(\mu) \approx \left(\log \frac{\mu_0}{\mu} \right)^{-m}, \quad (116)$$

where we neglect any constant prefactor to simplify the discussion. The coupling exhibits a log flow to zero with a power set by $m > 0$. Then the RG factor, defined via $n = Z_n^{-1/2} n_0$, gives the flow of the surface order,

$$\mu \frac{d}{d\mu} n(\mu) = \frac{N-1}{2\pi} g(\mu) n(\mu), \quad (117)$$

in which we have used the anomalous dimension in Eq. (111). This leads to the following solution for the surface order parameter

$$n(\mu) \approx \begin{cases} \exp \left[-\frac{N-1}{2\pi} \frac{1}{1-m} \left(\log \frac{\mu_0}{\mu} \right)^{1-m} \right], & m \neq 1 \\ \left(\frac{N-1}{2\pi} \log \frac{\mu_0}{\mu} \right)^{-1}, & m = 1 \end{cases} \quad (118)$$

If the g decays slowly with $m \leq 1$, the surface order parameter vanishes at the low-energy limit. In particular, it exhibits a logarithmic flow to zero when $m = 1$, which is exactly the case of extraordinary-log criticality. Only when g decays fast enough, $m > 1$, the surface order will remain finite in the long-wavelength limit, i.e., the surface orders! This happens at the extraordinary transition of the tricritical point as $m > 1$ in the RG flow given in Eq. (109).

Lastly, we comment on the relation between our result and the no-go theorem for the continuous symmetry breaking in the context of BCFT by Cuomo and Zhang in Ref. [22]. Cuomo and Zhang analyzed the Ward identity of a continuous internal symmetry (the $O(N)$ symmetry in our case) in BCFT. The Ward identity can be split into a bulk part and a boundary part. With a crucial assumption that the RG terminates at a fixed point, the continuous symmetry breaking would lead to a pole in the boundary spectral weight, which implies a decoupled sector of gapless Goldstone modes. Then the machinery of Coleman's theorem can be applied to argue the absence of symmetry breaking on the surface. In our case, such an assumption is not valid. More specifically, the marginal log flow for the bulk coupling constant couples to the boundary flow of the NLSM, which then renders an intriguing logarithmic flow with $m > 1$ for the NLSM coupling g . If we assumed the bulk RG terminates at the fixed point, which is a Gaussian fixed point, then the mean-field order parameter profile Eq. (46) and the mean-field Green's function Eq. (48) would not be correct. This would imply that the extraordinary transition does not exist, a conclusion that is widely regarded as incorrect [10, 11]. Hence, it is crucial to treat the boundary and bulk RG on an equal footing to reach a correct conclusion, which then falsifies the assumption in Ref. [22].

6 Conclusion

In this work, we have extended the understanding of the extraordinary transition in three-dimensional $O(N)$ boundary conformal field theories, focusing on the tricritical $O(N)$ model. By deriving the mean-field order parameter profile and propagator for general $|\vec{\phi}|^{2n}$ couplings and employing the technique of layer susceptibility, we constructed the boundary operator expansion (BOE) for the tricritical case ($n = 3$) at the one-loop level. Our results reveal the boundary operator spectrum and explore the extraordinary transition beyond the $O(N)$ model, showing that it exhibits an ordered boundary for any $N \geq 2$ in three dimensions. This exemplifies a scenario of continuous symmetry breaking in two dimensions under boundary criticality, in stark contrast to the critical $O(N)$ model with vanishing boundary orders. It arises because the upper critical dimension for the tricritical model is $d = 3$, leading to milder fluctuations compared to the critical $O(N)$ case.

Tricritical points emerge in ubiquitous systems, including ferroelectrics [60], liquid crystal [61–63] and polymer solutions [64]. When these systems are bounded by a boundary, which is unavoidable in the real world, it leads to fruitful boundary critical behaviors. While the ordinary and special transitions have been explored in Ref. [28], our work addresses the gaps in understanding the extraordinary transition. Realizations of the bulk tricritical point have been reported in Ref. [65, 66], also numerically verified in Ref. [64, 67–69]. It is worth emphasizing that the extraordinary transition needs no more fine-tuning parameters than the bulk tricritical point. Hence, we expect that our results can be tested in experiments. Finally, the methods and insights developed in this study lay a foundation for exploring BOEs in other models with higher-order couplings, thus opening avenues for further investigations into boundary criticality and its implications across diverse physical systems.

Acknowledgements

Funding information XS acknowledges the support from the Lavin-Bernick Grant during his visit to Tulane University, where the work was conducted. The work of S.-K. J. is supported by a start-up grant and a COR Research Fellowship from Tulane University.

A Properties of special functions

Here, we summarize the properties of Bessel function and Hypergeometric functions, which are used to calculate the Feynman diagram.

A.1 Determination of integral constants $C_1^{L,T}$

Define $Z_\nu(x) = e^{i\pi\nu} K_\nu(x)$, we have [70]

$$\begin{aligned} Z_{\nu-1}(x) - Z_{\nu+1}(x) &= \frac{2\nu}{x} Z_\nu(x), \\ Z_{\nu-1}(x) + Z_{\nu+1}(x) &= 2Z'_\nu(x) = \frac{2\nu}{x} Z_\nu(x) + 2Z_{\nu+1}(x). \end{aligned} \quad (119)$$

Therefore, the second property gives $e^{-i\pi} K_{\nu-1}(x) + e^{i\pi} K_{\nu+1}(x) = \frac{2\nu}{x} K_\nu(x) + 2e^{i\pi} K_{\nu+1}(x)$. The equation (39) can be simplified to

$$1 = -C_L p e^{-i\frac{n\pi}{1-n}} i x \left[K_{\alpha_L}(x) K_{\alpha_L+1}(-x) + K_{\alpha_L}(-x) K_{\alpha_L+1}(x) \right], \quad (120)$$

Moreover, defining $K_\nu(x) = \frac{1}{2}\pi i e^{i\frac{\nu\pi}{2}} H_\nu^{(1)}(e^{i\frac{\pi}{2}}x)$ and $K_\nu(e^{i\pi}x) = -\frac{1}{2}\pi i e^{-i\frac{\nu\pi}{2}} H_\nu^{(2)}(e^{i\frac{\pi}{2}}x)$, we have the property for $H_\nu^{(1)}$ and $H_\nu^{(2)}$ that [70]

$$H_{\nu+1}^{(1)}(x)H_\nu^{(2)}(x) - H_\nu^{(1)}(x)H_{\nu+1}^{(2)}(x) = -\frac{4i}{\pi x}. \quad (121)$$

Therefore, the equation (39) can be simplified to

$$\begin{aligned} 1 &= -C_L p e^{-i\frac{n\pi}{1-n}} i x \frac{\pi^2}{4} \left[e^{-i\frac{\pi}{2}} H_{\alpha_L}^{(1)}(e^{i\frac{\pi}{2}}x) H_{\alpha_L+1}^{(2)}(e^{i\frac{\pi}{2}}x) + e^{i\frac{\pi}{2}} H_{\alpha_L}^{(2)}(e^{i\frac{\pi}{2}}x) H_{\alpha_L+1}^{(1)}(e^{i\frac{\pi}{2}}x) \right] \\ &= C_L p e^{-i\frac{n\pi}{1-n}} x \frac{\pi^2}{4} \frac{-4i}{\pi x e^{i\frac{\pi}{2}}} = -\pi C_L p e^{-i\frac{n\pi}{1-n}}, \end{aligned} \quad (122)$$

A.2 Properties of regularized generalized hypergeometric function

The regularized generalized hypergeometric function ${}_p\tilde{F}_q[a, b, z]$ is related to the generalized hypergeometric function ${}_pF_q[a, b, z]$ that ${}_p\tilde{F}_q[a, b, z] = \frac{{}_pF_q[a, b, z]}{\Gamma(b_1)\cdots\Gamma(b_q)}$ with $a = \{a_1, \dots, a_p\}$ and $b = \{b_1, \dots, b_q\}$. The regularized generalized hypergeometric function is defined as

$${}_p\tilde{F}_q[a, b, z] = \sum_{k=0}^{\infty} \frac{\prod_{j=1}^p (a_j)_k}{\Gamma(k+1) \prod_{i=1}^q \Gamma(b_i+k)} z^k, \quad (123)$$

where $(a_j)_k = a_j(a_j+1)\dots(a_j+k-1) = \frac{\Gamma(a_j+k)}{\Gamma(a_j)}$ is the Pochhammer symbols.

In the main text, we use the integral property that

$$\int dz z^{\alpha-1} {}_p\tilde{F}_q[\{a_1, \dots, a_p\}, \{b_1, \dots, b_q\}, z] = \Gamma(\alpha) z^\alpha {}_{p+1}\tilde{F}_{q+1}[\{\alpha, a_1, \dots, a_p\}, \{\alpha+1, b_1, \dots, b_q\}, z]. \quad (124)$$

B Details of Feynman diagram calculation

In this section, we show the details of calculation for one-point and two-point functions shown in the main text.

B.1 Details of the evaluation for the integral $\int dp p^{d-2} I_\nu(pz) I_{\nu+1}(pz) K_\nu(pz') K_{\nu+1}(pz')$

First, we expand $I_\nu(pz) I_{\nu+1}(pz)$ with the polynomial of pz that [70]

$$I_\nu(pz) I_{\nu+1}(pz) = \left(\frac{1}{2}pz\right)^{2\nu+1} \sum_{k=0}^{\infty} \frac{(2\nu+k+2)_k \left(\frac{1}{2}pz\right)^{2k}}{k! \Gamma(\nu+k+1) \Gamma(\nu+k+2)}, \quad (125)$$

where $(a)_k = \Gamma(a+k)/\Gamma(a)$. Next, we perform the integration term by term and then sum over k , which gives

$$\begin{aligned}
& \int dp p^{d-2} I_\nu(pz) I_{\nu+1}(pz) K_\nu(pz') K_{\nu+1}(pz') \\
&= \sum_{k=0}^{\infty} \frac{(2\nu+k+2)_k (\frac{1}{2}z)^{2k+2\nu+1}}{k! \Gamma(\nu+k+1) \Gamma(\nu+k+2)} \int dp p^{d-2+2k+2\nu+1} K_\nu(pz') K_{\nu+1}(pz') \\
&= \sum_{k=0}^{\infty} \frac{(2\nu+k+2)_k (\frac{1}{2}z)^{2k+2\nu+1}}{k! \Gamma(\nu+k+1) \Gamma(\nu+k+2)} z'^{-d-2k-2\nu} \frac{\sqrt{\pi} \Gamma(\frac{d-2+2k+2\nu+1}{2} - \nu) \Gamma(\frac{d-2+2k+2\nu+1}{2} + \nu + 1) \Gamma(\frac{d-2+2k+2\nu+1}{2})}{4 \Gamma(\frac{1+d-2+2k+2\nu+1}{2})} \\
&= z'^{1-d} \frac{1}{4} \left(\frac{z}{z'}\right)^{1+2\nu} \Gamma\left(\frac{d-1}{2}\right) \Gamma\left(\frac{3+2\nu}{2}\right) \Gamma\left(\frac{d-1+2\nu}{2}\right) \Gamma\left(\frac{d+1+4\nu}{2}\right) \\
&\quad \times {}_4\tilde{F}_3\left[\left\{\frac{d-1}{2}, \frac{3+2\nu}{2}, \frac{d-1+2\nu}{2}, \frac{d+1+4\nu}{2}\right\}, \left\{2+\nu, \frac{d+2\nu}{2}, 2+2\nu\right\}, \left(\frac{z}{z'}\right)^2\right],
\end{aligned} \tag{126}$$

where ${}_p\tilde{F}_q$ is the regularized generalized hypergeometric function, ${}_p\tilde{F}_q[a, b, z] = \frac{{}_pF_q[a, b, z]}{\Gamma(b_1) \cdots \Gamma(b_q)}$ with $a = \{a_1, \dots, a_p\}$ and $b = \{b_1, \dots, b_q\}$.

B.2 Details of the evaluation for the integral I_1 and I_2

We present the detail of the evaluation for the integral I_1 and I_2 in Eq. 67. We make a coordinate transformation $Y = \frac{y_2}{y_1}$ in I_1 and $Y = \frac{y_1}{y_2}$ in I_2 to get

$$\begin{aligned}
I_1 &= \int_0^\infty dy_1 \int_{y_1}^\infty dy_2 \frac{1}{y_1 y_2} \frac{\min(z_1, y_1)}{\max(z_1, y_1)} \frac{\min(z_2, y_2)}{\max(z_2, y_2)} y_1^{3-d} \left(\frac{y_1}{y_2}\right)^{d+1} \\
&\quad \times {}_4\tilde{F}_3\left[\left\{\frac{d-1}{2}, \frac{5}{2}, \frac{d+1}{2}, \frac{d+5}{2}\right\}, \left\{3, \frac{d+2}{2}, 4\right\}, \left(\frac{y_1}{y_2}\right)^2\right] \\
&= \int_1^\infty dY Y^{-d-2} {}_4\tilde{F}_3\left[\left\{\frac{d-1}{2}, \frac{5}{2}, \frac{d+1}{2}, \frac{d+5}{2}\right\}, \left\{3, \frac{d+2}{2}, 4\right\}, Y^{-2}\right] \int_0^\infty dy_1 y_1^{2-d} \frac{\min(z_1, y_1)}{\max(z_1, y_1)} \frac{\min(\frac{z_2}{Y}, y_1)}{\max(\frac{z_2}{Y}, y_1)}. \\
I_2 &= \int_0^\infty dy_2 \int_{y_2}^\infty dy_1 \frac{1}{y_1 y_2} \frac{\min(z_1, y_1)}{\max(z_1, y_1)} \frac{\min(z_2, y_2)}{\max(z_2, y_2)} y_2^{3-d} \left(\frac{y_2}{y_1}\right)^{d+1} \\
&\quad \times {}_4\tilde{F}_3\left[\left\{\frac{d-1}{2}, \frac{5}{2}, \frac{d+1}{2}, \frac{d+5}{2}\right\}, \left\{3, \frac{d+2}{2}, 4\right\}, \left(\frac{y_2}{y_1}\right)^2\right] \\
&= \int_1^\infty dY Y^{-d-2} {}_4\tilde{F}_3\left[\left\{\frac{d-1}{2}, \frac{5}{2}, \frac{d+1}{2}, \frac{d+5}{2}\right\}, \left\{3, \frac{d+2}{2}, 4\right\}, Y^{-2}\right] \int_0^\infty dy_2 y_2^{2-d} \frac{\min(\frac{z_1}{Y}, y_2)}{\max(\frac{z_1}{Y}, y_2)} \frac{\min(z_2, y_2)}{\max(z_2, y_2)}.
\end{aligned}$$

In the following, we give the derivation for $z_1 < z_2$. The result for $z_1 > z_2$ can be obtained by exchanging z_1 and z_2 . So in the main text, we have the result for general z_1 and z_2 .

We can directly calculate that for $z_1 < z_2$,

$$\int_0^\infty dy y^{2-d} \frac{\min(z_1, y)}{\max(z_1, y)} \frac{\min(z_2, y)}{\max(z_2, y)} = z_1^{3-d} (A\zeta + B\zeta^{d-2}), \tag{127}$$

with $A = \frac{-2}{(d-5)(d-3)}$, $B = \frac{-2}{(d-3)(d-1)}$. Note that $\zeta = \frac{z_1}{z_2}$ in the above expression as $z_1 < z_2$.

Because $z_1 < z_2$ and $\zeta = \frac{z_1}{z_2} < 1$, the integral I_1 can be simplified as

$$\begin{aligned}
I_1 &= \int_1^\infty dY Y^{-d-2} {}_4\tilde{F}_3 \left[\left\{ \frac{d-1}{2}, \frac{5}{2}, \frac{d+1}{2}, \frac{d+5}{2} \right\}, \left\{ 3, \frac{d+2}{2}, 4 \right\}, Y^{-2} \right] \\
&\quad \times \left(\Theta(\zeta^{-1} - Y) z_1^{3-d} [A(\zeta Y) + B(\zeta Y)^{d-2}] + \Theta(Y - \zeta^{-1}) \left(\frac{z_2}{Y}\right)^{3-d} [A(\zeta Y)^{-1} + B(\zeta Y)^{-d+2}] \right) \\
&= \frac{z_1^{3-d}}{2} \int_{\zeta^2}^1 dy y^{\frac{d-1}{2}} {}_4\tilde{F}_3 \left[\left\{ \frac{d-1}{2}, \frac{5}{2}, \frac{d+1}{2}, \frac{d+5}{2} \right\}, \left\{ 3, \frac{d+2}{2}, 4 \right\}, y \right] \left(A\zeta y^{-\frac{1}{2}} + B\zeta^{d-2} y^{-\frac{d-2}{2}} \right) \\
&\quad + \frac{z_2^{3-d}}{2} \int_0^{\zeta^2} dy y^{\frac{d-1}{2} + \frac{3-d}{2}} {}_4\tilde{F}_3 \left[\left\{ \frac{d-1}{2}, \frac{5}{2}, \frac{d+1}{2}, \frac{d+5}{2} \right\}, \left\{ 3, \frac{d+2}{2}, 4 \right\}, y \right] \left(A\zeta^{-1} y^{\frac{1}{2}} + B\zeta^{-d+2} y^{\frac{d-2}{2}} \right),
\end{aligned} \tag{128}$$

where we have made a variable transformation $y = Y^{-2}$ in the second equality. To calculate it explicitly, we use the property of regularized generalized hypergeometric function that [71]

$$\int dz z^{\alpha-1} {}_p\tilde{F}_q [\{a_1, \dots, a_p\}, \{b_1, \dots, b_q\}, z] = \Gamma(\alpha) z^\alpha {}_{p+1}\tilde{F}_{q+1} [\{\alpha, a_1, \dots, a_p\}, \{\alpha+1, b_1, \dots, b_q\}, z]. \tag{129}$$

Therefore, the integral I_1 is

$$\begin{aligned}
I_1 &= \frac{z_1^{3-d}}{2} A\zeta \left[\Gamma\left(\frac{d}{2}\right) y^{\frac{d}{2}} {}_5\tilde{F}_4 \left[\left\{ \frac{d}{2}, \frac{d-1}{2}, \frac{5}{2}, \frac{d+1}{2}, \frac{d+5}{2} \right\}, \left\{ \frac{d+2}{2}, 3, \frac{d+2}{2}, 4 \right\}, y \right] \right]_{\zeta^2}^1 \\
&\quad + \frac{z_1^{3-d}}{2} B\zeta^{d-2} \left[\Gamma\left(\frac{3}{2}\right) y^{\frac{3}{2}} {}_5\tilde{F}_4 \left[\left\{ \frac{3}{2}, \frac{d-1}{2}, \frac{5}{2}, \frac{d+1}{2}, \frac{d+5}{2} \right\}, \left\{ \frac{5}{2}, 3, \frac{d+2}{2}, 4 \right\}, y \right] \right]_{\zeta^2}^1 \\
&\quad + \frac{z_2^{3-d}}{2} A\zeta^{-1} \left[\Gamma\left(\frac{5}{2}\right) y^{\frac{5}{2}} {}_5\tilde{F}_4 \left[\left\{ \frac{5}{2}, \frac{d-1}{2}, \frac{5}{2}, \frac{d+1}{2}, \frac{d+5}{2} \right\}, \left\{ \frac{7}{2}, 3, \frac{d+2}{2}, 4 \right\}, y \right] \right]_0^{\zeta^2} \\
&\quad + \frac{z_2^{3-d}}{2} B\zeta^{-d+2} \left[\Gamma\left(\frac{d+2}{2}\right) y^{\frac{d+2}{2}} {}_5\tilde{F}_4 \left[\left\{ \frac{d+2}{2}, \frac{d-1}{2}, \frac{5}{2}, \frac{d+1}{2}, \frac{d+5}{2} \right\}, \left\{ \frac{d+4}{2}, 3, \frac{d+2}{2}, 4 \right\}, y \right] \right]_0^{\zeta^2},
\end{aligned} \tag{130}$$

where $[f(y)]_a^b = f(b) - f(a)$. Following the same method, the integral I_2 in Eq. (127) can be evaluated. For simplicity, we do not show the explicit derivation and result. Now after both

integrals have been evaluated, the final result can be simplified further to get

$$\begin{aligned}
I_1 + I_2 = & \frac{z_1^{3-d}}{2} A \zeta \left\{ \Gamma\left(\frac{d}{2}\right) {}_5\tilde{F}_4\left[\left\{\frac{d}{2}, \frac{d-1}{2}, \frac{5}{2}, \frac{d+1}{2}, \frac{d+5}{2}\right\}, \left\{\frac{d+2}{2}, 3, \frac{d+2}{2}, 4\right\}, 1\right] \right. \\
& \left. + \Gamma\left(\frac{5}{2}\right) {}_5\tilde{F}_4\left[\left\{\frac{5}{2}, \frac{d-1}{2}, \frac{5}{2}, \frac{d+1}{2}, \frac{d+5}{2}\right\}, \left\{\frac{7}{2}, 3, \frac{d+2}{2}, 4\right\}, 1\right] \right\} \\
& + \frac{z_1^{3-d}}{2} B \zeta^{d-2} \left\{ \Gamma\left(\frac{3}{2}\right) {}_5\tilde{F}_4\left[\left\{\frac{3}{2}, \frac{d-1}{2}, \frac{5}{2}, \frac{d+1}{2}, \frac{d+5}{2}\right\}, \left\{\frac{5}{2}, 3, \frac{d+2}{2}, 4\right\}, 1\right] \right. \\
& \left. + \Gamma\left(\frac{d+2}{2}\right) {}_5\tilde{F}_4\left[\left\{\frac{d+2}{2}, \frac{d-1}{2}, \frac{5}{2}, \frac{d+1}{2}, \frac{d+5}{2}\right\}, \left\{\frac{d+4}{2}, 3, \frac{d+2}{2}, 4\right\}, 1\right] \right\} \\
& + \frac{z_1^{3-d}}{2} A \zeta^{d+1} \left\{ \Gamma\left(\frac{5}{2}\right) {}_5\tilde{F}_4\left[\left\{\frac{5}{2}, \frac{d-1}{2}, \frac{5}{2}, \frac{d+1}{2}, \frac{d+5}{2}\right\}, \left\{\frac{7}{2}, 3, \frac{d+2}{2}, 4\right\}, \zeta^2\right] \right. \\
& \left. - \Gamma\left(\frac{d}{2}\right) {}_5\tilde{F}_4\left[\left\{\frac{d}{2}, \frac{d-1}{2}, \frac{5}{2}, \frac{d+1}{2}, \frac{d+5}{2}\right\}, \left\{\frac{d+2}{2}, 3, \frac{d+2}{2}, 4\right\}, \zeta^2\right] \right\} \\
& + \frac{z_1^{3-d}}{2} B \zeta^{d+1} \left\{ \Gamma\left(\frac{d+2}{2}\right) {}_5\tilde{F}_4\left[\left\{\frac{d+2}{2}, \frac{d-1}{2}, \frac{5}{2}, \frac{d+1}{2}, \frac{d+5}{2}\right\}, \left\{\frac{d+4}{2}, 3, \frac{d+2}{2}, 4\right\}, \zeta^2\right] \right. \\
& \left. - \Gamma\left(\frac{3}{2}\right) {}_5\tilde{F}_4\left[\left\{\frac{3}{2}, \frac{d-1}{2}, \frac{5}{2}, \frac{d+1}{2}, \frac{d+5}{2}\right\}, \left\{\frac{5}{2}, 3, \frac{d+2}{2}, 4\right\}, \zeta^2\right] \right\}. \tag{131}
\end{aligned}$$

By incorporating the result for $z_1 > z_2$, and separating the expression according to the order of ζ , Eq. (67) will become

$$b'_{23} = \frac{90^{\frac{3}{2}}}{(6!)^2} \frac{S_{d-1}}{32(2\pi)^{d-1}} \sqrt{u_0(z_1 z_2)^{\frac{4-d}{2}}} \left(AC_1 \zeta^{\frac{5-d}{2}} + BC_2 \zeta^{\frac{d-1}{2}} \right) + (z_1 z_2)^{\frac{4-d}{2}} H_d(\zeta), \tag{132}$$

where the constants C_1 and C_2 are

$$\begin{aligned}
C_1 = & \Gamma\left(\frac{d-1}{2}\right) \Gamma\left(\frac{5}{2}\right) \Gamma\left(\frac{d+1}{2}\right) \Gamma\left(\frac{d+5}{2}\right) \\
& \times \left\{ \Gamma\left(\frac{d}{2}\right) {}_5\tilde{F}_4\left[\left\{\frac{d}{2}, \frac{d-1}{2}, \frac{5}{2}, \frac{d+1}{2}, \frac{d+5}{2}\right\}, \left\{\frac{d+2}{2}, 3, \frac{d+2}{2}, 4\right\}, 1\right] \right. \\
& \left. + \Gamma\left(\frac{5}{2}\right) {}_5\tilde{F}_4\left[\left\{\frac{5}{2}, \frac{d-1}{2}, \frac{5}{2}, \frac{d+1}{2}, \frac{d+5}{2}\right\}, \left\{\frac{7}{2}, 3, \frac{d+2}{2}, 4\right\}, 1\right] \right\}, \\
C_2 = & \Gamma\left(\frac{d-1}{2}\right) \Gamma\left(\frac{5}{2}\right) \Gamma\left(\frac{d+1}{2}\right) \Gamma\left(\frac{d+5}{2}\right) \\
& \times \left\{ \Gamma\left(\frac{3}{2}\right) {}_5\tilde{F}_4\left[\left\{\frac{3}{2}, \frac{d-1}{2}, \frac{5}{2}, \frac{d+1}{2}, \frac{d+5}{2}\right\}, \left\{\frac{5}{2}, 3, \frac{d+2}{2}, 4\right\}, 1\right] \right. \\
& \left. + \Gamma\left(\frac{d+2}{2}\right) {}_5\tilde{F}_4\left[\left\{\frac{d+2}{2}, \frac{d-1}{2}, \frac{5}{2}, \frac{d+1}{2}, \frac{d+5}{2}\right\}, \left\{\frac{d+4}{2}, 3, \frac{d+2}{2}, 4\right\}, 1\right] \right\}, \tag{133}
\end{aligned}$$

And the last term is explicitly given by

$$\begin{aligned}
H(\zeta) = & \frac{90^{\frac{3}{2}}}{(6!)^2} \frac{S_{d-1}}{32(2\pi)^{d-1}} \Gamma\left(\frac{d-1}{2}\right) \Gamma\left(\frac{5}{2}\right) \Gamma\left(\frac{d+1}{2}\right) \Gamma\left(\frac{d+5}{2}\right) \sqrt{u_0} \zeta^{\frac{d+5}{2}} \\
& \left\{ A \Gamma\left(\frac{5}{2}\right) {}_5\tilde{F}_4\left[\left\{\frac{5}{2}, \frac{d-1}{2}, \frac{5}{2}, \frac{d+1}{2}, \frac{d+5}{2}\right\}, \left\{\frac{7}{2}, 3, \frac{d+2}{2}, 4\right\}, \zeta^2\right] \right. \\
& - A \Gamma\left(\frac{d}{2}\right) {}_5\tilde{F}_4\left[\left\{\frac{d}{2}, \frac{d-1}{2}, \frac{5}{2}, \frac{d+1}{2}, \frac{d+5}{2}\right\}, \left\{\frac{d+2}{2}, 3, \frac{d+2}{2}, 4\right\}, \zeta^2\right] \\
& + B \Gamma\left(\frac{d+2}{2}\right) {}_5\tilde{F}_4\left[\left\{\frac{d+2}{2}, \frac{d-1}{2}, \frac{5}{2}, \frac{d+1}{2}, \frac{d+5}{2}\right\}, \left\{\frac{d+4}{2}, 3, \frac{d+2}{2}, 4\right\}, \zeta^2\right] \\
& \left. - B \Gamma\left(\frac{3}{2}\right) {}_5\tilde{F}_4\left[\left\{\frac{3}{2}, \frac{d-1}{2}, \frac{5}{2}, \frac{d+1}{2}, \frac{d+5}{2}\right\}, \left\{\frac{5}{2}, 3, \frac{d+2}{2}, 4\right\}, \zeta^2\right] \right\}. \tag{134}
\end{aligned}$$

with $A = \frac{-2}{(d-5)(d-3)}$, $B = \frac{-2}{(d-3)(d-1)}$.

B.3 Details of the evaluation for the integral $I'_{1,2}$ and $I''_{1,2}$

The evaluation of the integrals $I'_{1,2}$ is similar to $I_{1,2}$. Via a series of changes of variables and simplifications, the integral can be simplified into

$$\begin{aligned}
I'_1 &= \int_0^\infty dy_1 \int_{y_1}^\infty dy_2 \frac{1}{y_1 y_2} \left(\frac{\min(z_1, y_1)}{\max(z_1, y_1)} \right)^2 \left(\frac{\min(z_2, y_2)}{\max(z_2, y_2)} \right)^2 y_1^{3-d} \left(\frac{y_1}{y_2} \right)^{d+2} \\
&\quad \times {}_4\tilde{F}_3 \left[\left\{ \frac{5}{2}, \frac{d-1}{2}, \frac{d+3}{2}, \frac{d+7}{2} \right\}, \left\{ 3, 5, \frac{d+4}{2} \right\}, \left(\frac{y_1}{y_2} \right)^2 \right] \\
&= \frac{z_1^{3-d}}{2} \int_{\zeta^2}^1 dy y^{\frac{d}{2}} {}_4\tilde{F}_3 \left[\left\{ \frac{5}{2}, \frac{d-1}{2}, \frac{d+3}{2}, \frac{d+7}{2} \right\}, \left\{ 3, 5, \frac{d+4}{2} \right\}, y \right] \left(A' \zeta^{d-1} y^{-\frac{d-1}{2}} + B' \zeta^2 y^{-1} \right) \\
&\quad + \frac{z_2^{3-d}}{2} \int_0^{\zeta^2} dy y^{\frac{3}{2}} {}_4\tilde{F}_3 \left[\left\{ \frac{5}{2}, \frac{d-1}{2}, \frac{d+3}{2}, \frac{d+7}{2} \right\}, \left\{ 3, 5, \frac{d+4}{2} \right\}, y \right] \left(A' \zeta^{1-d} y^{\frac{d-1}{2}} + B' \zeta^{-2} y \right)
\end{aligned} \tag{135}$$

where, in the derivation, we have assumed $z_1 < z_2$. Using Eq. (129), we arrive at

$$\begin{aligned}
I'_1 &= \frac{z_1^{3-d}}{2} A' \zeta^{d-1} \left[\Gamma \left(\frac{3}{2} \right) y^{\frac{3}{2}} {}_5\tilde{F}_4 \left[\left\{ \frac{3}{2}, \frac{5}{2}, \frac{d-1}{2}, \frac{d+3}{2}, \frac{d+7}{2} \right\}, \left\{ \frac{5}{2}, 3, 5, \frac{d+4}{2} \right\}, y \right] \right]_{\zeta^2}^1 \\
&\quad + \frac{z_1^{3-d}}{2} B' \zeta^2 \left[\Gamma \left(\frac{d}{2} \right) y^{\frac{d}{2}} {}_5\tilde{F}_4 \left[\left\{ \frac{d}{2}, \frac{5}{2}, \frac{d-1}{2}, \frac{d+3}{2}, \frac{d+7}{2} \right\}, \left\{ \frac{d+2}{2}, 3, 5, \frac{d+4}{2} \right\}, y \right] \right]_{\zeta^2}^1 \\
&\quad + \frac{z_2^{3-d}}{2} A' \zeta^{1-d} \left[\Gamma \left(\frac{d+4}{2} \right) y^{\frac{d+4}{2}} {}_5\tilde{F}_4 \left[\left\{ \frac{d+4}{2}, \frac{5}{2}, \frac{d-1}{2}, \frac{d+3}{2}, \frac{d+7}{2} \right\}, \left\{ \frac{d+6}{2}, 3, 5, \frac{d+4}{2} \right\}, y \right] \right]_0^{\zeta^2} \\
&\quad + \frac{z_2^{3-d}}{2} B' \zeta^{-2} \left[\Gamma \left(\frac{7}{2} \right) y^{\frac{7}{2}} {}_5\tilde{F}_4 \left[\left\{ \frac{7}{2}, \frac{5}{2}, \frac{d-1}{2}, \frac{d+3}{2}, \frac{d+7}{2} \right\}, \left\{ \frac{9}{2}, 3, 5, \frac{d+4}{2} \right\}, y \right] \right]_0^{\zeta^2},
\end{aligned} \tag{136}$$

We skip the derivation for I'_2 for simplicity, as it is similar. The final result is given by

$$\begin{aligned}
I'_1 + I'_2 &= \frac{z_1^{3-d}}{2} A' \zeta^{d-1} \left[\Gamma \left(\frac{3}{2} \right) {}_5\tilde{F}_4 \left[\left\{ \frac{3}{2}, \frac{5}{2}, \frac{d-1}{2}, \frac{d+3}{2}, \frac{d+7}{2} \right\}, \left\{ \frac{5}{2}, 3, 5, \frac{d+4}{2} \right\}, 1 \right] \right. \\
&\quad \left. + \Gamma \left(\frac{d+4}{2} \right) {}_5\tilde{F}_4 \left[\left\{ \frac{d+4}{2}, \frac{5}{2}, \frac{d-1}{2}, \frac{d+3}{2}, \frac{d+7}{2} \right\}, \left\{ \frac{d+6}{2}, 3, 5, \frac{d+4}{2} \right\}, 1 \right] \right] \\
&\quad + \frac{z_1^{3-d}}{2} B' \zeta^2 \left[\Gamma \left(\frac{d}{2} \right) {}_5\tilde{F}_4 \left[\left\{ \frac{d}{2}, \frac{5}{2}, \frac{d-1}{2}, \frac{d+3}{2}, \frac{d+7}{2} \right\}, \left\{ \frac{d+2}{2}, 3, 5, \frac{d+4}{2} \right\}, 1 \right] \right. \\
&\quad \left. + \Gamma \left(\frac{7}{2} \right) {}_5\tilde{F}_4 \left[\left\{ \frac{7}{2}, \frac{5}{2}, \frac{d-1}{2}, \frac{d+3}{2}, \frac{d+7}{2} \right\}, \left\{ \frac{9}{2}, 3, 5, \frac{d+4}{2} \right\}, 1 \right] \right] \\
&\quad + \frac{z_1^{3-d}}{2} A' \zeta^{d+2} \left[\Gamma \left(\frac{d+4}{2} \right) {}_5\tilde{F}_4 \left[\left\{ \frac{d+4}{2}, \frac{5}{2}, \frac{d-1}{2}, \frac{d+3}{2}, \frac{d+7}{2} \right\}, \left\{ \frac{d+6}{2}, 3, 5, \frac{d+4}{2} \right\}, \zeta^2 \right] \right. \\
&\quad \left. - \Gamma \left(\frac{3}{2} \right) {}_5\tilde{F}_4 \left[\left\{ \frac{3}{2}, \frac{5}{2}, \frac{d-1}{2}, \frac{d+3}{2}, \frac{d+7}{2} \right\}, \left\{ \frac{5}{2}, 3, 5, \frac{d+4}{2} \right\}, \zeta^2 \right] \right] \\
&\quad + \frac{z_1^{3-d}}{2} B' \zeta^{d+2} \left[\Gamma \left(\frac{7}{2} \right) {}_5\tilde{F}_4 \left[\left\{ \frac{7}{2}, \frac{5}{2}, \frac{d-1}{2}, \frac{d+3}{2}, \frac{d+7}{2} \right\}, \left\{ \frac{9}{2}, 3, 5, \frac{d+4}{2} \right\}, \zeta^2 \right] \right. \\
&\quad \left. - \Gamma \left(\frac{d}{2} \right) {}_5\tilde{F}_4 \left[\left\{ \frac{d}{2}, \frac{5}{2}, \frac{d-1}{2}, \frac{d+3}{2}, \frac{d+7}{2} \right\}, \left\{ \frac{d+2}{2}, 3, 5, \frac{d+4}{2} \right\}, \zeta^2 \right] \right].
\end{aligned} \tag{137}$$

Note that this is the result for $z_1 < z_2$. The result for $z_1 > z_2$ can be obtained by exchanging z_1 and z_2 . With these integrals, the one-loop calculation for the layer susceptibility is

$$c'_{23} = \frac{90^{\frac{3}{2}}}{(6!)^2} \frac{S_{d-1}}{128(2\pi)^{d-1}} \sqrt{u_0(z_1 z_2)^{\frac{4-d}{2}}} \left(A' C'_1 \zeta^{\frac{d+1}{2}} + B' C'_2 \zeta^{\frac{7-d}{2}} \right) + (z_1 z_2)^{\frac{4-d}{2}} H'_d(\zeta), \quad (138)$$

where

$$\begin{aligned} C'_1 &= \Gamma\left(\frac{5}{2}\right) \Gamma\left(\frac{d-1}{2}\right) \Gamma\left(\frac{d+3}{2}\right) \Gamma\left(\frac{d+7}{2}\right) \\ &\times \left\{ \Gamma\left(\frac{3}{2}\right) {}_5\tilde{F}_4 \left[\left\{ \frac{3}{2}, \frac{5}{2}, \frac{d-1}{2}, \frac{d+3}{2}, \frac{d+7}{2} \right\}, \left\{ \frac{5}{2}, 3, 5, \frac{d+4}{2} \right\}, 1 \right] \right. \\ &\left. + \Gamma\left(\frac{d+4}{2}\right) {}_5\tilde{F}_4 \left[\left\{ \frac{d+4}{2}, \frac{5}{2}, \frac{d-1}{2}, \frac{d+3}{2}, \frac{d+7}{2} \right\}, \left\{ \frac{d+6}{2}, 3, 5, \frac{d+4}{2} \right\}, 1 \right] \right\}, \\ C'_2 &= \Gamma\left(\frac{5}{2}\right) \Gamma\left(\frac{d-1}{2}\right) \Gamma\left(\frac{d+3}{2}\right) \Gamma\left(\frac{d+7}{2}\right) \\ &\times \left\{ \Gamma\left(\frac{d}{2}\right) {}_5\tilde{F}_4 \left[\left\{ \frac{d}{2}, \frac{5}{2}, \frac{d-1}{2}, \frac{d+3}{2}, \frac{d+7}{2} \right\}, \left\{ \frac{d+2}{2}, 3, 5, \frac{d+4}{2} \right\}, 1 \right] \right. \\ &\left. + \Gamma\left(\frac{7}{2}\right) {}_5\tilde{F}_4 \left[\left\{ \frac{7}{2}, \frac{5}{2}, \frac{d-1}{2}, \frac{d+3}{2}, \frac{d+7}{2} \right\}, \left\{ \frac{9}{2}, 3, 5, \frac{d+4}{2} \right\}, 1 \right] \right\}, \end{aligned} \quad (139)$$

and

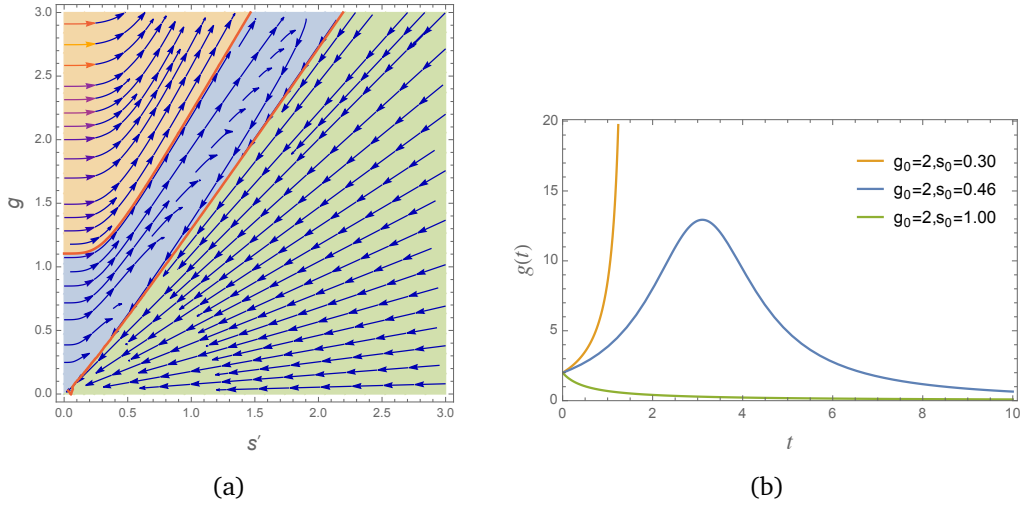
$$\begin{aligned} H'(\zeta) &= \frac{90^{\frac{3}{2}}}{(6!)^2} \frac{S_{d-1}}{128(2\pi)^{d-1}} \Gamma\left(\frac{5}{2}\right) \Gamma\left(\frac{d-1}{2}\right) \Gamma\left(\frac{d+3}{2}\right) \Gamma\left(\frac{d+7}{2}\right) \sqrt{u_0} \zeta^{\frac{d+7}{2}} \\ &\left\{ A' \Gamma\left(\frac{d+4}{2}\right) {}_5\tilde{F}_4 \left[\left\{ \frac{d+4}{2}, \frac{5}{2}, \frac{d-1}{2}, \frac{d+3}{2}, \frac{d+7}{2} \right\}, \left\{ \frac{d+6}{2}, 3, 5, \frac{d+4}{2} \right\}, \zeta^2 \right] \right. \\ &- A' \Gamma\left(\frac{3}{2}\right) {}_5\tilde{F}_4 \left[\left\{ \frac{3}{2}, \frac{5}{2}, \frac{d-1}{2}, \frac{d+3}{2}, \frac{d+7}{2} \right\}, \left\{ \frac{5}{2}, 3, 5, \frac{d+4}{2} \right\}, \zeta^2 \right] \\ &+ B' \Gamma\left(\frac{7}{2}\right) {}_5\tilde{F}_4 \left[\left\{ \frac{7}{2}, \frac{5}{2}, \frac{d-1}{2}, \frac{d+3}{2}, \frac{d+7}{2} \right\}, \left\{ \frac{9}{2}, 3, 5, \frac{d+4}{2} \right\}, \zeta^2 \right] \\ &\left. - B' \Gamma\left(\frac{d}{2}\right) {}_5\tilde{F}_4 \left[\left\{ \frac{d}{2}, \frac{5}{2}, \frac{d-1}{2}, \frac{d+3}{2}, \frac{d+7}{2} \right\}, \left\{ \frac{d+2}{2}, 3, 5, \frac{d+4}{2} \right\}, \zeta^2 \right] \right\}. \end{aligned} \quad (140)$$

The evaluation for $I''_{1,2}$ is similar, so we skip the derivation but present the final results. The layer susceptibility c'_{24} is

$$c'_{24} = \frac{90^{\frac{3}{2}}}{(6!)^2} \frac{S_{d-1}}{128(2\pi)^{d-1}} \sqrt{u_0(z_1 z_2)^{\frac{4-d}{2}}} \left(A' C''_1 \zeta^{\frac{d+1}{2}} + B' C''_2 \zeta^{\frac{7-d}{2}} \right) + (z_1 z_2)^{\frac{4-d}{2}} H''_d(\zeta), \quad (141)$$

where

$$\begin{aligned} C''_1 &= \Gamma\left(\frac{3}{2}\right) \Gamma\left(\frac{d-1}{2}\right) \Gamma\left(\frac{d+1}{2}\right) \Gamma\left(\frac{d+3}{2}\right) \\ &\times \left\{ \Gamma\left(\frac{1}{2}\right) {}_5\tilde{F}_4 \left[\left\{ \frac{1}{2}, \frac{3}{2}, \frac{d-1}{2}, \frac{d+1}{2}, \frac{d+3}{2} \right\}, \left\{ \frac{3}{2}, 2, 3, \frac{d+2}{2} \right\}, 1 \right] \right. \\ &\left. + \Gamma\left(\frac{d+2}{2}\right) {}_5\tilde{F}_4 \left[\left\{ \frac{d+2}{2}, \frac{3}{2}, \frac{d-1}{2}, \frac{d+1}{2}, \frac{d+3}{2} \right\}, \left\{ \frac{d+4}{2}, 2, 3, \frac{d+2}{2} \right\}, 1 \right] \right\}, \\ C''_2 &= \Gamma\left(\frac{3}{2}\right) \Gamma\left(\frac{d-1}{2}\right) \Gamma\left(\frac{d+1}{2}\right) \Gamma\left(\frac{d+3}{2}\right) \\ &\times \left\{ \Gamma\left(\frac{d-2}{2}\right) {}_5\tilde{F}_4 \left[\left\{ \frac{d-2}{2}, \frac{3}{2}, \frac{d-1}{2}, \frac{d+1}{2}, \frac{d+3}{2} \right\}, \left\{ \frac{d}{2}, 2, 3, \frac{d+2}{2} \right\}, 1 \right] \right. \\ &\left. + \Gamma\left(\frac{5}{2}\right) {}_5\tilde{F}_4 \left[\left\{ \frac{5}{2}, \frac{3}{2}, \frac{d-1}{2}, \frac{d+1}{2}, \frac{d+3}{2} \right\}, \left\{ \frac{7}{2}, 2, 3, \frac{d+2}{2} \right\}, 1 \right] \right\}, \end{aligned} \quad (142)$$

Figure 4: The phase diagram $g - s'$ of $N = 6$.

and

$$\begin{aligned}
H''(\zeta) = & \frac{90^{\frac{3}{2}}}{(6!)^2} \frac{S_{d-1}}{128(2\pi)^{d-1}} \Gamma\left(\frac{3}{2}\right) \Gamma\left(\frac{d-1}{2}\right) \Gamma\left(\frac{d+1}{2}\right) \Gamma\left(\frac{d+3}{2}\right) \sqrt{u_0} \zeta^{\frac{d+3}{2}} \\
& \left\{ A' \Gamma\left(\frac{d+2}{2}\right) {}_5\tilde{F}_4 \left[\left\{ \frac{d+2}{2}, \frac{3}{2}, \frac{d-1}{2}, \frac{d+1}{2}, \frac{d+3}{2} \right\}, \left\{ \frac{d+4}{2}, 2, 3, \frac{d+2}{2} \right\}, \zeta^2 \right] \right. \\
& - A' \Gamma\left(\frac{1}{2}\right) {}_5\tilde{F}_4 \left[\left\{ \frac{1}{2}, \frac{3}{2}, \frac{d-1}{2}, \frac{d+1}{2}, \frac{d+3}{2} \right\}, \left\{ \frac{3}{2}, 2, 3, \frac{d+2}{2} \right\}, \zeta^2 \right] \\
& + B' \Gamma\left(\frac{5}{2}\right) {}_5\tilde{F}_4 \left[\left\{ \frac{5}{2}, \frac{3}{2}, \frac{d-1}{2}, \frac{d+1}{2}, \frac{d+3}{2} \right\}, \left\{ \frac{7}{2}, 2, 3, \frac{d+2}{2} \right\}, \zeta^2 \right] \\
& \left. - B' \Gamma\left(\frac{d-2}{2}\right) {}_5\tilde{F}_4 \left[\left\{ \frac{d-2}{2}, \frac{3}{2}, \frac{d-1}{2}, \frac{d+1}{2}, \frac{d+3}{2} \right\}, \left\{ \frac{d}{2}, 2, 3, \frac{d+2}{2} \right\}, \zeta^2 \right] \right\}. \tag{143}
\end{aligned}$$

C Solution of the coupled RG equations Eq. (107)

Here we discuss the full solution of the RG equations Eq. (107). Defining $\mu = e^{-t}$, we can solve the RG equation and get $s(t)$ and $g(t)$ with initial condition s_0 and g_0 :

$$s(t) = (4at + s_0^4)^{1/4}, \quad g(t) = \frac{12ag_0}{\pi g_0(4at + s_0^4)^{3/2} - 12abg_0t + 12a - \pi g_0 s_0^6}, \tag{144}$$

where $a = \frac{3(3N+22)}{128\pi^4}$ and $b = \frac{n-2}{2\pi}$ are two constants. In general, for $t \rightarrow \infty$, $g(t) \rightarrow 0$, but there exist some initial conditions of s_0 and g_0 such that $g(t_0)^{-1} = 0$ for a finite $t_0 > 0$. This is equivalent to that the two functions (of t) $\pi g_0(4at + s_0^4)^{3/2}$ and $12abg_0t - 12a + \pi g_0 s_0^6$ are tangent to each other. It leads to $t_0 = \frac{4b^2/\pi^2 - s_0^4}{4a}$ and $g_0 = \frac{12a\pi^2}{(\pi s_0^2 - 2b)^2(\pi s_0^2 + b)}$. Since we do not consider the divergent case, $t_0 < 0$ requires $s_0^2 > \frac{2b}{\pi}$. Because the perturbative coupling is $s' = gs$, we can plot the phase diagram of $g - s'$, which is shown in Fig. 4 (a) with $N = 6$. The orange region corresponds to the parameter (g, s') that will flow to $1/g = 0$, the green region corresponds to g that directly flows to zero, which is given by Eq. (109), and the blue region corresponds to the region where g will first flow to a larger value, and then flow to zero, which is shown in Fig. 4 (b). Notice that g flows to a large value means the RG result is not valid. Hence, we only consider the green region in this paper.

D Correlation function of the critical $O(N)$ theory

In this section, we use our general method to calculate the correlation function of the scalar ϕ^4 theory. We only consider the result of the most complicate Feynman diagram, which will give the same result as Ref. [10] Eq. (3.13).

Starting from Eq. (3.6) in Ref. [10]

$$\chi(z, z') = \frac{u_0^2}{2} \int_0^\infty dy \int_0^\infty dy' G_0(p=0; z, y) m_0(y) \left[\int dr G_0^2(r; , y, y') \right] m_0(y') G_0(p=0; y', z'), \quad (145)$$

with $m_0(z) = \sqrt{\frac{12}{u_0}} \frac{1}{z}$. With $n = 2$ for ϕ^4 theory and $\alpha_L = \frac{3}{2} + 1 = \frac{5}{2}$ in Eq. (43), we have

$$G_0(p; z, z') = \sqrt{zz'} I\left(\frac{5}{2}, pz\right) K\left(\frac{5}{2}, pz'\right) \quad (146)$$

for $z < z'$, and $G_0(p=0; z, z') = \frac{1}{5} \frac{\min(z, z')^3}{\max(z, z')^2} = \frac{1}{5} \sqrt{zz'} \zeta^{\frac{5}{2}}$.

Therefore, with the method above, assuming $z < z'$ and $\zeta = \frac{z}{z'}$, we have

$$b^L(z, z') = \frac{S_{d-1}}{(2\pi)^{d-1}} z z' \frac{1}{4} z^5 z'^{-d-4} \Gamma\left(\frac{d-1}{2}\right) \Gamma(3) \Gamma\left(\frac{d+4}{2}\right) \Gamma\left(\frac{d+9}{2}\right) \times {}_4\tilde{F}_3\left[\left\{\frac{d-1}{2}, 3, \frac{d+4}{2}, \frac{d+9}{2}\right\}, \left\{\frac{7}{2}, \frac{d+5}{2}, 6\right\}, \left(\frac{z}{z'}\right)^2\right]. \quad (147)$$

Plugging it into $\chi(z, z')$, we have

$$\chi(z, z') = \frac{6u_0}{25} \frac{1}{4} \frac{S_{d-1}}{(2\pi)^{d-1}} \Gamma\left(\frac{d-1}{2}\right) \Gamma(3) \Gamma\left(\frac{d+4}{2}\right) \Gamma\left(\frac{d+9}{2}\right) (I_1 + I_2), \quad (148)$$

where $I_{1,2}$, which is not shown explicitly, are integrals of regularized hypergeometric function, and can be done with

$$\int_0^\infty dy y^{2-d} \frac{\min(z_1, y)^3}{\max(z_1, y)^2} \frac{\min(z_2, y)^3}{\max(z_2, y)^2} = z_2^{5-d} (A'' \zeta^{7-d} + B'' \zeta^3), \quad (149)$$

for $z_1 < z_2$ and $\zeta = \frac{z_1}{z_2}$. Here $A'' = \frac{-5}{(4-d)(9-d)}$ and $B'' = \frac{5}{(4-d)(1+d)}$. Importantly, because z_1 and z_2 are symmetric, we can just exchange them for $z_2 < z_1$. Therefore, we arrive at

$$\chi(z, z') = \frac{6u_0}{25} \frac{S_{d-1}}{(2\pi)^{d-1}} z'^{5-d} \zeta^3 \left(\frac{A'' \tilde{C}_1}{8} \zeta^{4-d} + \frac{B'' \tilde{C}_2}{8} + h(\zeta) \right). \quad (150)$$

where we define \tilde{C}_1 and \tilde{C}_2 that

$$\begin{aligned} \tilde{C}_1 = & \Gamma\left(\frac{d-1}{2}\right) \Gamma(3) \Gamma\left(\frac{d+4}{2}\right) \Gamma\left(\frac{d+9}{2}\right) \\ & \times \left(\Gamma\left(\frac{d}{2}\right) {}_5\tilde{F}_4\left[\left\{\frac{d}{2}, \frac{d-1}{2}, 3, \frac{d+4}{2}, \frac{d+9}{2}\right\}, \left\{\frac{d+2}{2}, \frac{7}{2}, \frac{d+5}{2}, 6\right\}, 1\right] \right. \\ & \left. + \Gamma\left(\frac{9}{2}\right) {}_5\tilde{F}_4\left[\left\{\frac{9}{2}, \frac{d-1}{2}, 3, \frac{d+4}{2}, \frac{d+9}{2}\right\}, \left\{\frac{11}{2}, \frac{7}{2}, \frac{d+5}{2}, 6\right\}, y\right] \right), \end{aligned} \quad (151)$$

$$\begin{aligned} \tilde{C}_2 = & \Gamma\left(\frac{d-1}{2}\right) \Gamma(3) \Gamma\left(\frac{d+4}{2}\right) \Gamma\left(\frac{d+9}{2}\right) \\ & \times \left(\Gamma(2) {}_5\tilde{F}_4\left[\left\{2, \frac{d-1}{2}, 3, \frac{d+4}{2}, \frac{d+9}{2}\right\}, \left\{3, \frac{7}{2}, \frac{d+5}{2}, 6\right\}, 1\right] \right. \\ & \left. + \Gamma\left(\frac{d+5}{2}\right) {}_5\tilde{F}_4\left[\left\{\frac{d+5}{2}, \frac{d-1}{2}, 3, \frac{d+4}{2}, \frac{d+9}{2}\right\}, \left\{\frac{d+7}{2}, \frac{7}{2}, \frac{d+5}{2}, 6\right\}, 1\right] \right). \end{aligned} \quad (152)$$

And

$$\begin{aligned}
 h(\zeta) = & \frac{1}{4} \Gamma\left(\frac{d-1}{2}\right) \Gamma(3) \Gamma\left(\frac{d+4}{2}\right) \Gamma\left(\frac{d+9}{2}\right) \\
 & \times \left(\frac{A''}{2} \zeta^4 \Gamma\left(\frac{9}{2}\right) {}_5\tilde{F}_4 \left[\left\{ \frac{9}{2}, \frac{d-1}{2}, 3, \frac{d+4}{2}, \frac{d+9}{2} \right\}, \left\{ \frac{11}{2}, \frac{7}{2}, \frac{d+5}{2}, 6 \right\}, \zeta^2 \right] \right. \\
 & + \frac{B''}{2} \zeta^4 \Gamma\left(\frac{d+5}{2}\right) {}_5\tilde{F}_4 \left[\left\{ \frac{d+5}{2}, \frac{d-1}{2}, 3, \frac{d+4}{2}, \frac{d+9}{2} \right\}, \left\{ \frac{d+7}{2}, \frac{7}{2}, \frac{d+5}{2}, 6 \right\}, \zeta^2 \right] \\
 & - \frac{A''}{2} \zeta^4 \Gamma\left(\frac{d}{2}\right) y^{\frac{d}{2}} {}_5\tilde{F}_4 \left[\left\{ \frac{d}{2}, \frac{d-1}{2}, 3, \frac{d+4}{2}, \frac{d+9}{2} \right\}, \left\{ \frac{d+2}{2}, \frac{7}{2}, \frac{d+5}{2}, 6 \right\}, \zeta^2 \right] \\
 & \left. - \frac{B''}{2} \zeta^4 \Gamma(2) {}_5\tilde{F}_4 \left[\left\{ 2, \frac{d-1}{2}, 3, \frac{d+4}{2}, \frac{d+9}{2} \right\}, \left\{ 3, \frac{7}{2}, \frac{d+5}{2}, 6 \right\}, \zeta^2 \right] \right). \quad (153)
 \end{aligned}$$

To compare the results with Eq. (3.13) in Ref. [10], we need to simplify \tilde{C}_1 and \tilde{C}_2 in Eq. (151) and Eq. (152), which are divergent for $d \rightarrow 4$. To expand them around $d = 4 - \epsilon$, by definition, we rewrite them with the summation form that

$$\tilde{C}_1 = 2^{6-d} \sum_{k=0}^{\infty} \left[\frac{(k+1)(k+\frac{d+7}{2})(k+\frac{d+5}{2})(k+\frac{d+9}{2})(k+\frac{d+2}{2})}{(k+5)(k+4)(k+3)(k+\frac{5}{2})(k+\frac{9}{2})} - 1 \right] \frac{\Gamma(2k+d-1)}{\Gamma(2k+4)} + 2^{6-d} \sum_{k=0}^{\infty} \frac{\Gamma(2k+d-1)}{\Gamma(2k+4)}, \quad (154)$$

where we have used $\Gamma(z)\Gamma(z+\frac{1}{2}) = 2^{1-2z} \sqrt{\pi} \Gamma(2z)$. In the second line, we separate it into two parts because the first part is finite for $d \rightarrow 4$, but the second term is $2^{6-d} \sum_{k=0}^{\infty} \frac{\Gamma(2k+d-1)}{\Gamma(2k+4)} \approx \frac{2}{\epsilon}$. And we can get the leading term of \tilde{C}_2 similarly.

In Ref. [10], for $z < z'$, they give that

$$\begin{aligned}
 \chi(z, z') = & \frac{1}{5} \frac{z^3}{z'^2} \frac{24}{5} u_0 \frac{S_d^{-1}}{d-2} 2^{2-d} z'^{4-d} \left[\frac{\zeta^{4-d} K}{9-d} + \frac{L - \zeta^{4-d} K}{4-d} + \frac{L}{d+1} + H_d(\zeta) \right] \\
 = & \frac{6}{25} u_0 z'^{5-d} \zeta^3 \frac{S_{d-1}}{(2\pi)^{d-1}} 2^{3-d} \Gamma(d-2) [A'' K \zeta^{4-d} + B'' L + H_d(\zeta)]. \quad (155)
 \end{aligned}$$

where we use $\frac{S_d^{-1}}{d-2} 2^{4-d} \cdot \frac{(2\pi)^{d-1}}{S_{d-1}} = \frac{2^{3-d}}{d-2} \Gamma(d-1)$. A'' and B'' are defined in Eq. (149), and K and L are

$$K = \frac{(2-\epsilon)(72-\epsilon^2)}{6\epsilon(2+\epsilon)(4+\epsilon)(6+\epsilon)}, \quad L = \frac{(2-\epsilon)(4-\epsilon)(6-\epsilon)}{48\epsilon(2+\epsilon)}, \quad (156)$$

where $\epsilon = 4 - d$. The function $H_d(\zeta)$ is a complicated function, which is not shown here.

To prove the equality of two results, we just need to check that $2^{3-d} \Gamma(d-2) K = \frac{\tilde{C}_1}{8}$, $2^{3-d} \Gamma(d-2) L = \frac{\tilde{C}_2}{8}$ and $2^{3-d} \Gamma(d-2) H_d(\zeta) = h(\zeta)$. Although it is challenging to prove them, we can find that $2^{3-d} \Gamma(d-2) K = \frac{\tilde{C}_1}{8}$ and $2^{3-d} \Gamma(d-2) L = \frac{\tilde{C}_2}{8}$ are valid up to $\mathcal{O}(\epsilon^2)$. Also, $2^{3-d} \Gamma(d-2) H_d(\zeta) = h(\zeta)$ is valid up to $\mathcal{O}(\zeta^{22})$. It would be interesting to give a rigorous proof of these relations in the future.

References

- [1] N. Andrei *et al.*, *Boundary and Defect CFT: Open Problems and Applications*, J. Phys. A **53**(45), 453002 (2020), doi:[10.1088/1751-8121/abb0fe](https://doi.org/10.1088/1751-8121/abb0fe), [1810.05697](https://arxiv.org/abs/1810.05697).
- [2] J. L. Cardy, *Conformal invariance and surface critical behavior*, Nuclear Physics B **240**(4), 514 (1984), doi:[https://doi.org/10.1016/0550-3213\(84\)90241-4](https://doi.org/10.1016/0550-3213(84)90241-4).

- [3] D. McAvity and H. Osborn, *Conformal field theories near a boundary in general dimensions*, Nuclear Physics B **455**(3), 522 (1995), doi:[https://doi.org/10.1016/0550-3213\(95\)00476-9](https://doi.org/10.1016/0550-3213(95)00476-9).
- [4] P. Liendo, L. Rastelli and B. C. van Rees, *The Bootstrap Program for Boundary CFT_d*, JHEP **07**, 113 (2013), doi:[10.1007/JHEP07\(2013\)113](https://doi.org/10.1007/JHEP07(2013)113), [1210.4258](https://arxiv.org/abs/1210.4258).
- [5] H. Diehl and S. Dietrich, *Field-theoretical approach to static critical phenomena in semi-infinite systems*, Zeitschrift für Physik B Condensed Matter **42**(1), 65 (1981).
- [6] H. Diehl, *Field-theory of surface critical behaviour*, Phase transitions and and Critical Phenomena, edited by C. Domb and JL Lebowitz **10**, 75 (1986).
- [7] T. C. Lubensky and M. H. Rubin, *Critical phenomena in semi-infinite systems. ii. mean-field theory*, Phys. Rev. B **12**, 3885 (1975), doi:[10.1103/PhysRevB.12.3885](https://doi.org/10.1103/PhysRevB.12.3885).
- [8] J. Rudnick and D. Jasnow, *Critical wall perturbations: Scaling and renormalization group*, Phys. Rev. Lett. **49**, 1595 (1982), doi:[10.1103/PhysRevLett.49.1595](https://doi.org/10.1103/PhysRevLett.49.1595).
- [9] E. Eisenriegler and M. Stapper, *Critical behavior near a symmetry-breaking surface and the stress tensor*, Phys. Rev. B **50**, 10009 (1994), doi:[10.1103/PhysRevB.50.10009](https://doi.org/10.1103/PhysRevB.50.10009).
- [10] M. A. Shpot, *Boundary conformal field theory at the extraordinary transition: The layer susceptibility to $O(\epsilon)$* , Journal of High Energy Physics **2021**(1) (2021), doi:[10.1007/jhep01\(2021\)055](https://doi.org/10.1007/jhep01(2021)055).
- [11] P. Dey, T. Hansen and M. Shpot, *Operator expansions, layer susceptibility and two-point functions in BCFT*, Journal of High Energy Physics **2020**(12) (2020), doi:[10.1007/jhep12\(2020\)051](https://doi.org/10.1007/jhep12(2020)051).
- [12] A. J. Bray and M. A. Moore, *Critical behaviour of semi-infinite systems*, Journal of Physics A: Mathematical and General **10**(11), 1927 (1977), doi:[10.1088/0305-4470/10/11/021](https://doi.org/10.1088/0305-4470/10/11/021).
- [13] H. W. Diehl and M. Smock, *Critical behavior at supercritical surface enhancement: Temperature singularity of surface magnetization and order-parameter profile to one-loop order*, Phys. Rev. B **47**, 5841 (1993), doi:[10.1103/PhysRevB.47.5841](https://doi.org/10.1103/PhysRevB.47.5841).
- [14] T. W. Burkhardt and H. W. Diehl, *Ordinary, extraordinary, and normal surface transitions: Extraordinary-normal equivalence and simple explanation of $|T - T_c|^{2-\alpha}$ singularities*, Phys. Rev. B **50**, 3894 (1994), doi:[10.1103/PhysRevB.50.3894](https://doi.org/10.1103/PhysRevB.50.3894).
- [15] H. W. Diehl, *Why boundary conditions do not generally determine the universality class for boundary critical behavior*, The European Physical Journal B **93**, 1 (2020).
- [16] M. A. Metlitski, *Boundary criticality of the $O(N)$ model in $d = 3$ critically revisited*, SciPost Phys. **12**, 131 (2022), doi:[10.21468/SciPostPhys.12.4.131](https://doi.org/10.21468/SciPostPhys.12.4.131).
- [17] F. Parisen Toldin, *Boundary critical behavior of the three-dimensional heisenberg universality class*, Phys. Rev. Lett. **126**, 135701 (2021), doi:[10.1103/PhysRevLett.126.135701](https://doi.org/10.1103/PhysRevLett.126.135701).
- [18] M. Hu, Y. Deng and J.-P. Lv, *Extraordinary-log surface phase transition in the three-dimensional xy model*, Phys. Rev. Lett. **127**, 120603 (2021), doi:[10.1103/PhysRevLett.127.120603](https://doi.org/10.1103/PhysRevLett.127.120603).

- [19] J. Padayasi, A. Krishnan, M. A. Metlitski, I. A. Gruzberg and M. Meineri, *The extraordinary boundary transition in the 3d $O(N)$ model via conformal bootstrap*, SciPost Phys. **12**, 190 (2022), doi:[10.21468/SciPostPhys.12.6.190](https://doi.org/10.21468/SciPostPhys.12.6.190).
- [20] X. Zou, S. Liu and W. Guo, *Surface critical properties of the three-dimensional clock model*, Phys. Rev. B **106**, 064420 (2022), doi:[10.1103/PhysRevB.106.064420](https://doi.org/10.1103/PhysRevB.106.064420).
- [21] A. Krishnan and M. A. Metlitski, *A plane defect in the 3d $O(N)$ model*, SciPost Phys. **15**, 090 (2023), doi:[10.21468/SciPostPhys.15.3.090](https://doi.org/10.21468/SciPostPhys.15.3.090).
- [22] G. Cuomo and S. Zhang, *Spontaneous symmetry breaking on surface defects*, JHEP **03**, 022 (2024), doi:[10.1007/JHEP03\(2024\)022](https://doi.org/10.1007/JHEP03(2024)022), [2306.00085](https://arxiv.org/abs/2306.00085).
- [23] H. Diehl and S. Dietrich, *Multicritical behaviour at surfaces*, Zeitschrift für Physik B Condensed Matter **50**(2), 117 (1983).
- [24] H. Diehl and M. Shpot, *Massive field-theory approach to surface critical behavior in three-dimensional systems*, Nuclear Physics B **528**(3), 595 (1998), doi:[https://doi.org/10.1016/S0550-3213\(98\)00489-1](https://doi.org/10.1016/S0550-3213(98)00489-1).
- [25] des Cloizeaux, J., *The lagrangian theory of polymer solutions at intermediate concentrations*, J. Phys. France **36**(4), 281 (1975), doi:[10.1051/jphys:01975003604028100](https://doi.org/10.1051/jphys:01975003604028100).
- [26] K. Binder and D. Landau, *Multicritical phenomena at surfaces*, Surface Science **61**(2), 577 (1976), doi:[https://doi.org/10.1016/0039-6028\(76\)90068-6](https://doi.org/10.1016/0039-6028(76)90068-6).
- [27] Duplantier, B., *Lagrangian tricritical theory of polymer chain solutions near the θ -point*, J. Phys. France **43**(7), 991 (1982), doi:[10.1051/jphys:01982004307099100](https://doi.org/10.1051/jphys:01982004307099100).
- [28] W. Speth, *Tricritical phase transitions in semi-infinite systems*, Zeitschrift für Physik B Condensed Matter **51**(4), 361 (1983).
- [29] G. Gumbs, *Analysis of the effect of surfaces on the tricritical behavior of systems*, Journal of Mathematical Physics **24**(1), 202 (1983).
- [30] E. Eisenriegler, *Universal amplitude ratios for the surface tension of polymer solutions*, The Journal of Chemical Physics **81**(10), 4666 (1984), doi:[10.1063/1.447401](https://doi.org/10.1063/1.447401), https://pubs.aip.org/aip/jcp/article-pdf/81/10/4666/18951020/4666_1_online.pdf.
- [31] Duplantier, B., *Direct or dimensional renormalizations of the tricritical polymer theory*, J. Phys. France **47**(5), 745 (1986), doi:[10.1051/jphys:01986004705074500](https://doi.org/10.1051/jphys:01986004705074500).
- [32] H. W. Diehl and E. Eisenriegler, *Walks, polymers, and other tricritical systems in the presence of walls or surfaces*, Europhysics Letters **4**(6), 709 (1987), doi:[10.1209/0295-5075/4/6/012](https://doi.org/10.1209/0295-5075/4/6/012).
- [33] B. Kutlu, A. Özkan, N. Seferoğlu, A. Solak and B. E. Binal, *The tricritical behavior of the 3d blume-capel model on a cellular automaton*, International Journal of Modern Physics C **16**, 933 (2005).
- [34] C. P. Herzog and N. Kobayashi, *The $O(N)$ model with ϕ^6 potential in $\mathbb{R}^2 \times \mathbb{R}^+$* , JHEP **09**, 126 (2020), doi:[10.1007/JHEP09\(2020\)126](https://doi.org/10.1007/JHEP09(2020)126), [2005.07863](https://arxiv.org/abs/2005.07863).
- [35] T. Grover, D. N. Sheng and A. Vishwanath, *Emergent Space-Time Supersymmetry at the Boundary of a Topological Phase*, Science **344**(6181), 280 (2014), doi:[10.1126/science.1248253](https://doi.org/10.1126/science.1248253), [1301.7449](https://arxiv.org/abs/1301.7449).

- [36] Z.-X. Li, Y.-F. Jiang and H. Yao, *Edge quantum criticality and emergent supersymmetry in topological phases*, Phys. Rev. Lett. **119**, 107202 (2017), doi:[10.1103/PhysRevLett.119.107202](https://doi.org/10.1103/PhysRevLett.119.107202).
- [37] L. Zhang and F. Wang, *Unconventional surface critical behavior induced by a quantum phase transition from the two-dimensional affleck-kennedy-lieb-tasaki phase to a néel-ordered phase*, Phys. Rev. Lett. **118**, 087201 (2017), doi:[10.1103/PhysRevLett.118.087201](https://doi.org/10.1103/PhysRevLett.118.087201).
- [38] X.-C. Wu, Y. Xu, H. Geng, C.-M. Jian and C. Xu, *Boundary criticality of topological quantum phase transitions in two-dimensional systems*, Phys. Rev. B **101**, 174406 (2020), doi:[10.1103/PhysRevB.101.174406](https://doi.org/10.1103/PhysRevB.101.174406).
- [39] R. Ma, L. Zou and C. Wang, *Edge physics at the deconfined transition between a quantum spin Hall insulator and a superconductor*, SciPost Phys. **12**, 196 (2022), doi:[10.21468/SciPostPhys.12.6.196](https://doi.org/10.21468/SciPostPhys.12.6.196).
- [40] R. Verresen, R. Thorngren, N. G. Jones and F. Pollmann, *Gapless topological phases and symmetry-enriched quantum criticality*, Phys. Rev. X **11**, 041059 (2021), doi:[10.1103/PhysRevX.11.041059](https://doi.org/10.1103/PhysRevX.11.041059).
- [41] X.-J. Yu, R.-Z. Huang, H.-H. Song, L. Xu, C. Ding and L. Zhang, *Conformal boundary conditions of symmetry-enriched quantum critical spin chains*, Phys. Rev. Lett. **129**, 210601 (2022), doi:[10.1103/PhysRevLett.129.210601](https://doi.org/10.1103/PhysRevLett.129.210601).
- [42] X.-J. Yu, S. Yang, H.-Q. Lin and S.-K. Jian, *Universal entanglement spectrum in one-dimensional gapless symmetry protected topological states*, Phys. Rev. Lett. **133**, 026601 (2024), doi:[10.1103/PhysRevLett.133.026601](https://doi.org/10.1103/PhysRevLett.133.026601).
- [43] X. Shen, Z. Wu and S.-K. Jian, *New boundary criticality in topological phases*, arXiv preprint arXiv:2407.15916 (2024).
- [44] Z. Zhou and Y. Zou, *Studying the 3d ising surface cfts on the fuzzy sphere*, arXiv preprint arXiv:2407.15914 (2024).
- [45] M. Dedushenko, *Ising bcft from fuzzy hemisphere*, arXiv preprint arXiv:2407.15948 (2024).
- [46] A. Karch and L. Randall, *Locally localized gravity*, JHEP **05**, 008 (2001), doi:[10.1088/1126-6708/2001/05/008](https://doi.org/10.1088/1126-6708/2001/05/008), [hep-th/0011156](https://arxiv.org/abs/hep-th/0011156).
- [47] A. Karch and L. Randall, *Open and closed string interpretation of SUSY CFT's on branes with boundaries*, JHEP **06**, 063 (2001), doi:[10.1088/1126-6708/2001/06/063](https://doi.org/10.1088/1126-6708/2001/06/063), [hep-th/0105132](https://arxiv.org/abs/hep-th/0105132).
- [48] T. Takayanagi, *Holographic Dual of BCFT*, Phys. Rev. Lett. **107**, 101602 (2011), doi:[10.1103/PhysRevLett.107.101602](https://doi.org/10.1103/PhysRevLett.107.101602), [1105.5165](https://arxiv.org/abs/1105.5165).
- [49] M. Fujita, T. Takayanagi and E. Tonni, *Aspects of AdS/BCFT*, JHEP **11**, 043 (2011), doi:[10.1007/JHEP11\(2011\)043](https://doi.org/10.1007/JHEP11(2011)043), [1108.5152](https://arxiv.org/abs/1108.5152).
- [50] T. Azeyanagi, A. Karch, T. Takayanagi and E. G. Thompson, *Holographic calculation of boundary entropy*, JHEP **03**, 054 (2008), doi:[10.1088/1126-6708/2008/03/054](https://doi.org/10.1088/1126-6708/2008/03/054), [0712.1850](https://arxiv.org/abs/0712.1850).
- [51] Y. Ge and S.-K. Jian, *Defect conformal field theory from sachdev-ye-kitaev interactions*, Phys. Rev. Lett. **133**, 266503 (2024), doi:[10.1103/PhysRevLett.133.266503](https://doi.org/10.1103/PhysRevLett.133.266503).

- [52] X. Sun and S.-K. Jian, *Holographic weak measurement*, JHEP **12**, 157 (2023), doi:[10.1007/JHEP12\(2023\)157](https://doi.org/10.1007/JHEP12(2023)157), [2309.15896](https://arxiv.org/abs/2309.15896).
- [53] X. Sun and S.-K. Jian, *Holographic dual of defect cft with corner contributions*, arXiv preprint arXiv:2407.19003 (2024).
- [54] E. Eisenriegler and H. W. Diehl, *Surface critical behavior of tricritical systems*, Phys. Rev. B **37**, 5257 (1988), doi:[10.1103/PhysRevB.37.5257](https://doi.org/10.1103/PhysRevB.37.5257).
- [55] P. M. Morse and H. Feshbach, *Methods of theoretical physics*, Technology Press (1946).
- [56] K. Ohno and Y. Okabe, *The $1/n$ expansion for the extraordinary transition of semi-infinite system*, Progress of Theoretical Physics **72**(4), 736 (1984), doi:[10.1143/PTP.72.736](https://doi.org/10.1143/PTP.72.736), <https://academic.oup.com/ptp/article-pdf/72/4/736/5241446/72-4-736.pdf>.
- [57] E. Brézin and J. Zinn-Justin, *Spontaneous breakdown of continuous symmetries near two dimensions*, Phys. Rev. B **14**, 3110 (1976), doi:[10.1103/PhysRevB.14.3110](https://doi.org/10.1103/PhysRevB.14.3110).
- [58] M. Moshe and J. Zinn-Justin, *Quantum field theory in the large n limit: a review*, Physics Reports **385**(3), 69 (2003), doi:[https://doi.org/10.1016/S0370-1573\(03\)00263-1](https://doi.org/10.1016/S0370-1573(03)00263-1).
- [59] J. Padayasi, A. Krishnan, M. A. Metlitski, I. A. Gruzberg and M. Meineri, *The extraordinary boundary transition in the 3d $O(N)$ model via conformal bootstrap*, SciPost Phys. **12**(6), 190 (2022), doi:[10.21468/SciPostPhys.12.6.190](https://doi.org/10.21468/SciPostPhys.12.6.190), [2111.03071](https://arxiv.org/abs/2111.03071).
- [60] A. Gordon, *Tricritical phase transitions in ferroelectrics*, Physica B+C **122**(3), 321 (1983), doi:[https://doi.org/10.1016/0378-4363\(83\)90059-1](https://doi.org/10.1016/0378-4363(83)90059-1).
- [61] B. M. Ocko, R. J. Birgeneau, J. D. Litster and M. E. Neubert, *Critical and tricritical behavior at the nematic to smectic-A transition*, Phys. Rev. Lett. **52**, 208 (1984), doi:[10.1103/PhysRevLett.52.208](https://doi.org/10.1103/PhysRevLett.52.208).
- [62] J. T. H. Marynissen and W. V. Dael, *Experimental evidence for a nematic to smectic a tricritical point in alkylcyanobiphenyl mixtures*, Molecular Crystals and Liquid Crystals **124**(1), 195 (1985), doi:[10.1080/00268948508079476](https://doi.org/10.1080/00268948508079476), <https://doi.org/10.1080/00268948508079476>.
- [63] T. Khalilov, D. Makarov and D. Petrov, *Tricritical phenomena and cascades of temperature phase transitions in a ferromagnetic liquid crystal suspension*, Crystals **11**(6) (2021), doi:[10.3390/cryst11060639](https://doi.org/10.3390/cryst11060639).
- [64] B. Duplantier and H. Saleur, *Exact tricritical exponents for polymers at the Θ point in two dimensions*, Phys. Rev. Lett. **59**, 539 (1987), doi:[10.1103/PhysRevLett.59.539](https://doi.org/10.1103/PhysRevLett.59.539).
- [65] M. A. Anisimov, A. F. Kostko and J. V. Sengers, *Competition of mesoscales and crossover to tricriticality in polymer solutions*, Phys. Rev. E **65**, 051805 (2002), doi:[10.1103/PhysRevE.65.051805](https://doi.org/10.1103/PhysRevE.65.051805).
- [66] J. Hager, M. Anisimov, J. Sengers and E. Gorodetskii, *Scaling of demixing curves and crossover from critical to tricritical behavior in polymer solutions*, The Journal of chemical physics **117**(12), 5940 (2002).
- [67] Baumgärtner, A., *Collapse of a polymer: evidence for tricritical behaviour in two dimensions*, J. Phys. France **43**(9), 1407 (1982), doi:[10.1051/jphys:019820043090140700](https://doi.org/10.1051/jphys:019820043090140700).

- [68] A. L. Owczarek and T. Prellberg, *First-order scaling near a second-order phase transition: Tricritical polymer collapse*, Europhysics Letters **51**(6), 602 (2000), doi:[10.1209/epl/i2000-00380-5](https://doi.org/10.1209/epl/i2000-00380-5).
- [69] K. Binder, W. Paul, T. Strauch, F. Rampf, V. Ivanov and J. Luettmmer-Strathmann, *Phase transitions of single polymer chains and of polymer solutions: insights from monte carlo simulations*, Journal of Physics: Condensed Matter **20**(49), 494215 (2008), doi:[10.1088/0953-8984/20/49/494215](https://doi.org/10.1088/0953-8984/20/49/494215).
- [70] *NIST Digital Library of Mathematical Functions*, <https://dlmf.nist.gov/>, Release 1.2.2 of 2024-09-15, F. W. J. Olver, A. B. Olde Daalhuis, D. W. Lozier, B. I. Schneider, R. F. Boisvert, C. W. Clark, B. R. Miller, B. V. Saunders, H. S. Cohl, and M. A. McClain, eds.
- [71] W. R. Inc., *The mathematical functions site*, <http://functions.wolfram.com/07.32.21.0002.01>, Champaign, IL, 2024.